C.P. No 137
(15,437 15,524)
A R C Technical Report

MINISTRY OF SUPPLY

AERONAUTICAL RESEARCH COUNCIL

CURRENT PAPERS

Pressure Distribution and Boundary Layer Investigations on 44 degree Swept-back Tapered Wing

Part I

Three-dimensional Tests on the Wing

Part II

Two-dimensional Pressure Distribution Tests

on 10 per cent Thick Symmetrical Aerofoil Section

By

Joseph Black, Ph D.,
University of Bristol,
Department of Aeronautical Engineering

LONDON . HER MAJESTY'S STATIONERY OFFICE

1953

Price 8s 6d net

Addendum to Part I

August, 1953

Laminar Boundary Layer Separation

In this report the term "bubble vortex" (Sect. 6.1. et seq.) has been used to describe the rotating mass of air lying parallel to the leading edge near the aerofoil nose under the separated boundary layer. It is now felt that the use of vortex in this context is misleading, since the air movement in the "bubble" may not resemble that in a true vortex. The term "separation bubble" is therefore suggested to replace "bubble vortex" whenever it occurs in the text.

Liquid Film Studies (Sect. 6.4.)

The interpretation of the liquid film patterns has been discussed with Mr. A. B. Haines and Dr. D. Küchemann of the R.A.E., and also by the Performance Sub-Committee of the Aeronautical Research Council. When this report was written, it was assumed that the liquid film moved over the wing surface solely under the influence of the shear stress imposed upon it by the traction of the boundary layer flow above; it has now been suggested that the film may also follow pressure gradients existing on the wing surface. The particular conditions which favour one influence more than the other have not yet been established, but some work is at present in progress which, it is hoped, will reveal the main factors controlling the movement of liquid films.

Interpretations made in this paper of the liquid film pattern should therefore be regarded at present as tentative only. Some of the unusual features of the liquid flow may possibly be attributable to the specific behaviour of the liquid film, without necessarily implying the existence of similar flow characteristics in the air boundary layer itself.

C. P. No. 137.

Pressure Distribution and Boundary Layer Investigations on a 44° Sweptback Tapered Wing

- By -
Joseph Black, Ph.D.,
University of Bristol,
Department of Aeronautical Engineering.

Part I
Three-dimensional Tests on the Wing

22nd December, 1952

SUMMARY

An experimental investigation of the aerodynamic characteristics of a tapered wing with a leading edge sweptback 44° has been carried out in a wind tunnel at a Reynolds number of 0.5×10^6, based on a mean chord of 10 in.

Chordwise pressure distributions at a number of spanwise locations were measured over a range of incidence. Considerable attention was given to investigating the boundary layer, quantitative measurements being made with a novel form of yawmeter head, and the flow being studied visually using wool tufts. In addition, a technique for revealing the direction of flow and formation of vortices in the layer was developed; this consists of spraying the wing with a suspension of lamp-black in paraffin with the wind off and then turning the wind on rapidly.

One of the most important results established was the relation of the unstable break in the pitching moment curve at a moderate value of overall lift coefficient to the initiation of stalling at the tip region. Another interesting feature was the formation of a "bubble" vortex lying parallel to the leading edge of the wing at low incidences, under the separated laminar layer. At higher incidences, complex vortex patterns were discovered, and the initial stalling at the wing tip was found to be associated in some way with the growth and inward movement of a standing vortex, with axis normal to the surface, which forms on the leading edge.

Contents/

Contents

List of Figures/

List of Figures

List of Symbols/

List of Symbols

s — semi-span

c — section chord

$c_{av} = \frac{S}{b}$ = wing average chord

$\bar{c} = \frac{\int_0^{b/2} c^2 dy}{\int_0^{b/2} c\,dy}$ = mean aerodynamic chord

S — wing area

y — length normal to plane-of-symmetry

Λ — angle of sweepback

$C_p = \frac{p_{loc} - p}{q}$ = pressure coefficient

p — static pressure

q — dynamic head of free stream

c_n — section normal-force coefficient

c_m — section pitching moment coefficient, about section leading edge

$\bar{C}_n$ — overall normal-force coefficient

$\bar{C}_{m_{\bar{c}/4}}$ — overall pitching moment coefficient, about wing mean quarter-chord point

$\frac{c_n c}{c_{av}}$ — loading coefficient, at some particular value of $\bar{C}_n$

$\frac{c_n c}{\bar{C}_n c_{av}}$ — loading coefficient, general

H — total head

h/c — chordwise location of centre-of-pressure

β — angle of cut-off of yawmeter head

$\eta = \frac{y}{b/2}$ non-dimensional lateral co-ordinate

1./

1. Introduction

The effect of increase in angle of incidence on the aerodynamic behaviour of a sweptback wing in incompressible flow is now well known. At some moderate value of the overall lift coefficient, well below $C_{L\ max}$, there may be a considerable decrease in slope of the $C_m - C_L$ curve, where the pitching-moment coefficient, C_m, is usually taken about the lateral axis through the wing mean quarter-chord point. With some planforms there may even be a change of sign of slope. Numerous pressure distribution tests and tuft studies have indicated that this coincides with the onset of stalling at the tip section, the region of stalling advancing inboard with increase of incidence. Sections inboard of the stalled region not only do not stall, but in some cases increase their lift-curve slope.

Various explanations of the phenomenon of tip stalling and its associated effect on pitching moment have been advanced, such as the increased aerodynamic loading which is produced outboard on a sweptback wing, or the outward drift of the boundary layer towards the tip, with consequent thickening and separation.

In the course of an investigation of the aerodynamic characteristics of a sweptback tapered wing, certain features of the pressure distributions suggested the existence of some unusual flow conditions in the boundary layer. Attention was therefore directed to an examination of the boundary layer flow with a view to relating its behaviour to the changes in the overall characteristics of the wing.

This paper describes first the results from the pressure distribution tests, and then deals with the investigation of the boundary layer and the development of the stalling on the wing.

The tests were carried out during 1951 and early 1952.

2. Details of Model and Tests

The wing tested was a semi-span model of that used on the D.H.108 (Fig.1). The main features were leading edge sweepback 44°, aspect ratio 4.3, taper ratio 0.326. The aerofoil section was symmetrical with a maximum thickness of 10% at 40% of the chord; from leading edge to maximum thickness the section was elliptic, and from there to the trailing edge it was quintic, with a 14° trailing edge angle. (Section ordinates are given in Table 1.) Twenty-three pressure holes were distributed round the line-of-flight chords at eight spanwise locations (Table 2).

For reasons connected with the main part of the investigation of the wing, (not described here), the model was made of solid Perspex.

All tests were carried out in a $3\frac{1}{2}$ ft diameter open-jet atmospheric-pressure working section return flow wind tunnel, at a wind speed of 103 ft/sec corresponding to a Reynolds number, based on a mean aerodynamic chord of 10.7 in., of 0.575×10^6.

For boundary layer measurement an arrowhead, or Conrad, yawmeter was used, in conjunction with a micrometer-traversing gear. Since this work was carried out, the use of a similar instrument has been reported (Ref.1). The head consisted of two hypodermic tubes, 0.06 in. outside diameter, soldered together and ground off to form an arrowhead; the angle of cut-off used was 45°. This angle produced a linear variation of pressure difference between the tubes with inclination, over an angular range of ±15°; Brebner (Ref.1) used a cut-off angle of 55° which increased the sensitivity, but reduced the linear range to ±10° of inclination.

The/

The total head recorded with one tube, H', when the head was aligned along the flow was found to bear the following relation to the free-stream total head H:

$$H' = H \times \cos^2 \beta$$

where β is the angle of cut-off. This is in accord with a simple analysis based on a resolution of flow velocities.

3. Pressure Distributions on the Wing

3.1 Chordwise Pressure Distributions and Isobars

3.1.1 Pressure Distribution at 0.83 Semi-span

The effect of increase in incidence on the pressure distribution at one particular spanwise location can be seen from Fig.2. An increase of incidence from 0° to 6° produces a large suction at the nose which continues to grow to a maximum at 9°. At 12° this peak suction at the nose falls away, but there is a general increase of suction farther aft over the section; the resultant distribution is almost triangular. The collapse of the nose suction does not indicate stalling, since the normal force is still increasing with incidence. With further increase in incidence, the pressure over the forward region of the section becomes almost constant, and at 18° the distribution is flat over the whole section.

These pressure distributions resemble those obtained in two-dimensional tests of thin aerofoils by Gault and McCullough[2]. The contrast in character between these distributions and those of a conventional round-nosed aerofoil may therefore arise as much from the inherent properties of the section as from the three-dimensional effects of sweepback (see Part II of this report).

The maximum positive pressure coefficient attained is 0.52, compared with unity at the stagnation point of a straight wing. Since the leading edge is swept back 44°, this confirms simple sweep theory, which predicts that the pressure coefficients will vary as $\cos^2 \Lambda$, where Λ is the sweepback angle.

3.1.2 Pressure Distributions at Other Spanwise Locations

The chordwise distributions at the various spanwise stations are presented isometrically on the wing planform in Fig.3(a) to 3(f), for incidences from 0° to 18°. The isobars are also included in these figures.

At 6° incidence (Fig.3(b)) all stations have well-developed peak suctions, but that at the root section is both smaller and further aft than the others. The maximum value appears towards the tip. The isobars, on the whole, lie along the constant percentage chord lines, except near the root leading edge where they curve round to lie normal to the line-of-flight.

Increase of incidence to 9° produces extremely high peak suctions about 0.75 semi-span, which fall away rapidly inboard and outboard. At the tip, the distribution exhibits an unusual build-up of suction towards the trailing edge. The isobars spread apart as they approach the tip.

At 12° (Fig.3(d)) there are three distinct regions, in each of which the forms of the distributions differ. The root chord has lost its peak suction, and what remains is followed by a narrow "dip" of increased pressure. The centre distributions are still well peaked, but at 0.93 semi-span the distribution is transitional to the "triangular" form existing at the tip.

Increase to 15° leaves the root chord distribution almost unchanged in form: the dip has been replaced by a small region of constant pressure. Only the sections between 0.2 and 0.56 semi-span retain a peak suction near the nose. The "triangular" distribution is now located at 0.68 semi-span, and outboard of this station the distributions get progressively flatter.

At/

At the highest incidence, 18°, (Fig. 3(f)) the peaks are confined to a narrow region between 0.2 and 0.44 semi-span.

3.1.3 Pressure Distributions in Tip Region

Chordwise pressure distributions over the sections near and at the tip reveal an interesting phenomenon when compared directly. In Fig.4 it will be seen that at 9° the tip section has a pronounced negative pressure rise from about 0.7 chord to the trailing edge. With increase of incidence, this spreads forward, so that at 11° there is increased negative pressure, compared with the inner sections, from about 0.4 chord. At 12° the effect is lessening, and at 15° the section is completely stalled.

This aft suction peak at the tip has been noted by Weber[3]; with an untapered 53° sweptback wing it appeared at 4° incidence and was found to be dependent on tip shape. A square tip produced a more marked peak. Babister[4] has also commented on the phenomenon, which arose on a 45° sweptback untapered wing at 12° incidence. Küchemann, Weber and Brebner[5] noted its existence in tests on a 45° sweptback wing and suggested that it arose from the rolling up of a vortex sheet along the trailing edge of the wing.

3.2 Spanwise Pressure Distributions

The pressure distributions along the constant percentage chord lines at the leading edge, 0.05 and 0.1 of the chord, are shown in Fig.5.

Along the leading edge, the pressure coefficients at zero incidence have the constant value of 0.52 along the whole semi-span, only decreasing at the tip section where the backward curvature begins. Thus the simple "cos² sweep angle" rule mentioned above appears to hold along the whole span. This is confirmed by other results: Dannenberg[6] recorded a C_{p_o} of 0.5 with 45° sweepback, and Wick[7] obtained a C_{p_o} of 0.2 with 63.4° sweepback. Weber and Brebner, with a complete wing as distinct from a semi-span model, obtained a C_{p_o} of unity at the wing apex, which fell to the "cos²" value at 0.08 semi-span.

With increase of incidence to 6° the growth of suction over the outboard span may be seen. At 9° the distribution along the leading edge is marked by a peak suction at 0.8 semi-span, with another lesser one at the tip itself.

The distribution at 12° is similar in form, but the peak suction is increased and occurs further inboard, about 0.6 semi-span. This inward movement of the peak suction continues with increase of incidence, until at 18° it is in the region of 0.25 semi-span.

4. Normal Forces on the Wing

4.1 Results from Investigation of Pressure Distributions

The variations of the local normal force coefficients c_n with incidence are shown in Fig.6; these coefficients were obtained by integration of the pressure distributions. The $c_n - \alpha$ curves are only linear at all the stations up to an incidence of about 6°. Above this incidence the slope at stations 0.025, 0.195 and 0.97 semi-span increases, the sections between remaining linear. At 12° the tip section reaches a $c_{n_{max}}$ of 0.54, while the sections at 0.195 and 0.44 semi-span increase their slope. Stalling progresses inwards from the tip; 12.5° for 0.93 semi-span, 14.5° for 0.83, 15.5° for 0.68. At the maximum incidence tested, 18°, the inboard sections remained unstalled.

The slopes of the $c_n - \alpha$ curves (over the linear range) rise from 0.037 per degree at the root to a maximum of 0.062 at 0.7 semi-span, then fall smoothly to 0.037 at the tip (Fig.7). The two-dimensional slope for the aerofoil section of the wing is 0.063 per degree (see Part II of this report).

Fig.8 shows the spanwise distribution of the normal force coefficient c_n. At 6° the maximum c_n occurs about 0.75 semi-span. The effect at 9° of localized increase in suction over the rear of the tip section shows up as a recovery in c_n close to the tip. At the higher incidences the maximum c_n occurs further inboard, until at 18° it is at mid semi-span.

Since/

Since the section normal force coefficient, c_n, is based on the local chord, the curves of Fig.8 do not show the loading on the wing. To obtain this, the local c_n must be based on the wing average chord, c_{av}, equal to Area/Span, giving the loading coefficients $c_n c/c_{av}$. These are shown in Fig.9. The relative decrease in c_n over the inboard sections at low incidence is compensated for by the larger chord, hence the loading is more evenly distributed along the span. Above 12°, when the tip loses lift, the combined effect of increased c_n and increased chord produces a large load inboard.

Integration of the loading coefficients over the span gives the overall normal force coefficient $\bar{C}_n$. The curves of Fig.9 may then be compared directly by plotting in terms of $c_n c/\bar{C}_n c_{av}$, which is done in Fig.10. The points for 6°, 9° and 12° lie close to each other, and the mean line through them may be taken as the non-dimensional loading on the wing in the sub-stalling incidence range.

The overall normal force curve is shown in Fig.11. There is only a slight decrease of slope towards 18°, the slope in the linear range being 0.049 per degree.

4.2 Comparison with Theoretical Predictions

The wing characteristics were calculated theoretically, using the Weissinger[8], Stanton-Jones[9] and Diederich[10] methods, since these are rapid and convenient to use.

4.2.1 Span Loading Distribution

The span loadings are tabulated below and plotted in Fig.10.

Span Location $\frac{y}{b/2}$	Measured	Weissinger	Stanton-Jones	Diederich
0	1.07	1.198	1.194	1.20
0.383	1.17	1.151	1.170	1.15
0.707	0.99	0.944	0.954	0.91
0.924	0.58	0.560	0.538	0.48

It will be seen that the Weissinger method gives too high a loading at the centre and underestimates the load outboard. The decreased loading measured at the centre may arise from the platform mounting of the semi-span model, but other tests with complete models of sweptback wings have also indicated this decrease in loading towards the root. Results from the Stanton-Jones method agree quite well with those of the Weissinger method, the points if plotted giving almost the identical curve: this is not surprising, since the method is based on numerous Weissinger solutions. To a certain extent, the same applies to the Diederich method, in that he bases his "ideal" distribution curves on lifting surface results.

4.2.2 Spanwise Location of Centre-of-pressure

All the methods predict the spanwise location of the overall centre-of-pressure of the wing very well.

	Measured	Weissinger	Stanton-Jones	Diederich
$\eta_{c.p}$	0.44	0.439	0.438	0.435

4.2.3/

4.2.3 Position of Aerodynamic Centre

Because the Weissinger method gives an accurate prediction of the spanwise location of the centre-of-pressure, it should give a good prediction of the longitudinal position of the aerodynamic centre. This is assumed to be the quarter-chord point of the line-of-flight chord lying along the location of the spanwise centre-of-pressure, $\eta_{c.p.}$.

Using the value of $\eta_{c.p.}$ of 0.439 from the last section gives the chordwise location of the aerodynamic centre as 0.29 $\bar{c}$, compared to the experimental value of 0.325 $\bar{c}$.

Hopkins (Ref.11) found the same measure of disagreement over his range of planforms; he improved the accuracy of the prediction by assuming the chordwise location of the aerodynamic centre to be at 25% of a chord normal to the sweep reference line, rather than a line-of-flight chord. When applied to the test wing, the theoretical position of the aerodynamic centre moved back to 0.335 $\bar{c}$, which is a slightly more accurate prediction.

	Measured	$\frac{1}{4}$c pt. Line-of-flight Chord	$\frac{1}{4}$c pt. Normal to Sweep Axis Chord
Aero Centre % M.A.C.	0.325	0.290	0.335

4.2.4 Lift-curve Slope

The measured and predicted values of lift-curve slope $\frac{dC_n}{d\alpha}$ were as follows:-

	Measured	Weissinger
$\frac{dC_n}{d\alpha}$	0.05	0.057

While this measure of agreement may seem reasonable, it differs from other results in that the theoretical prediction is usually lower than the measured value. Thus van Dorn and DeYoung[12] obtained the following values for an almost similar wing:

	Experiment	Weissinger	Falkner
$\frac{dC_L}{d\alpha}$	0.0538	0.047	0.0509

They noted that this bad agreement was the exoeption, the other planforms with less sweep showing much better agreement.

On the other hand, DeYoung[13] has plotted theoretical and experimental lift-curve slopes for a large collection of planforms, and the result for the test wing does lie within the general scatter, though admittedly it is on the opposite side of the line of perfect correlation to most of the highly swept planforms.

5./

5. Pitching Moments on the Wing

The curves of section pitching moment about the section leading edge are included in Fig.6. The range for which the moment varies linearly with incidence decreases from 18° at the root to only 5° at the tip. At incidences beyond the linear range, but still below stalling, there is a marked increase in stability, which appears to be associated with the local increase in $dc_m/d\alpha$. When the section stalls, an unstable moment is produced; thus at 18° sections inboard of 0.68 semi-span are increasingly stable, while those outboard have gone unstable.

The ratio of the sectional coefficients, c_m/c_n, gives the chordwise position of the local centre-of-pressure. (In the linear range this position also corresponds to the aerodynamic centre.) The spanwise distribution of this location, h/c, is shown in Fig.12. At low incidence the local centre-of-pressure at the root is located about 0.35 c aft of the leading edge, but lies along the quarter-chord line over the mid semi-span; in the tip region it goes forward to about 0.16 c. At 9° the change in tip conditions causes the centre-of-pressure to shift back slightly; stalling of the outboard sections is marked by a backward shift to about 0.4 c.

The variation with $\bar{C}_n$ of the overall pitching moment coefficient for the wing, taken about the lateral axis through the quarter-chord point of the mean aerodynamic chord, is shown in Fig.13. If negative slope is taken as indicating stability, the wing is stable up to a $\bar{C}_n$ of 0.45, with a small region of instability about a $\bar{C}_n$ of 0.6, corresponding to an incidence of 12°. Above a $\bar{C}_n$ of 0.7, the wing becomes markedly unstable, owing to the loss of lift at the tip, which is well behind the reference axis, and the corresponding increase of lift of the root sections ahead.

The small instability region coinciding with the onset of tip stalling at 12° was at first suspected, especially as these pitching moments are the result of overall integrations. Its existence was indirectly confirmed by a study of numerous balance test results for various sweptback wings, which revealed the same small break in the curves. This suggests the initiation of some phenomenon common to all the planforms tested, which is associated with the onset of the tip stall.

6. Boundary Layer and Stalling Behaviour

6.1 Indications from Pressure Measurements

The two-dimensional characteristics of thin aerofoils with a small nose radius have been investigated by Gault and McCullough[2]. Their results are discussed in detail in Part II of this report, but briefly they found that about 4° - 6° incidence the laminar boundary layer over the nose of the section separated, became transitional away from the surface, and re-attached further aft as a turbulent layer. Under the separated layer a "bubble" vortex is formed, which rotates about an axis parallel to the leading edge, so that at the side adjacent to the surface the flow is towards the leading edge. The presence of the laminar separation is indicated by a localized constant pressure region in the pressure distribution diagrams.

Stalling of the section resulted from failure of the separated transitional boundary layer to re-attach to the surface.

In an attempt to detect whether a similar phenomenon was occurring in the three-dimensional flow over the test wing, pressure measurements were made at 0.01, 0.025 and 0.05 of the chord at span locations of 0.32 and 0.88 semi-span. The results are shown in Fig.14.

At the inboard station the localized constant pressure indication appears between 0.025 and 0.05 c at 6°. A marked localized pressure recovery between 0.01 and 0.02 c exists at 9° and 12°, but disappears at 15°. Outboard a similar constant pressure region occurs at 6° and a pressure dip is present at 12°. Similar features were exhibited by the root section at 12° and 15° (Fig.3).

Plotting/

Plotting these results as variation of pressure at constant chord positions with incidence (Fig.15) indicates an intersection of the curves for 0.025 and 0.05 chord at 6° incidence at the inboard location; this suggests laminar separation at this point. A similar intersection at the same incidence at 0.88 semi-span also suggests that the vortex extends spanwise.

The contrast in unstalled and stalled behaviour at the two span locations shows up clearly; inboard at 15° the negative pressures continue to increase with incidence, but outboard from about 10° onwards the pressures at all chordwise positions recover and decrease along a common path.

6.2 Boundary Layer Measurements

Measurements of the boundary layer were made at 0.2 and 0.8 of the chord at various spanwise locations. Typical results are shown in Fig.16 for x/c of 0.8 at 0.44 semi-span. The increase in the thickness of the layer with incidence is considerable; it grows from about 0.005 c at 0° to 0.04 c at 12°, and to 0.10 c at 15°. At 18° the layer appears to be separating.

The magnitude of the spanwise velocity component is indicated by the flow deflection measured through the layer. At 12° incidence the flow is deflected outwards through 15°, and at 18° this increases to over 30°, the flow then lying almost parallel to the wing trailing edge. The greatest part of the deflection occurs very close to the surface, the free stream remaining relatively unaffected.

The layer was found to thicken with movement outboard along the span, and also approached separation, as indicated by a steepening profile, at a progressively earlier incidence.

Measurements near the leading edge at low incidence indicated a thin boundary layer with no appreciable deflection. Above 12° the yawmeter did not give consistent readings, even when rotated through ±20°. No reason for this sudden failure of response was then apparent.

6.3 Tuft Studies

Fig.17 shows tuft behaviour as incidence is increased. Deflection of the tufts outwards becomes appreciable near the trailing edge about mid semi-span at 9° incidence. The outward deflection is very firmly established at 12°, the rear tufts streaming parallel to the trailing edge, with the exception of one just inboard of the 0.44 semi-span chord. All tufts along the tip chord are agitated, and those near the leading edge appear to swing forward.

With further increase of incidence (15° and 18°) the outward deflection is marked even to the root chord and the outboard tufts are very agitated, suggesting separated flow. In spite of their disorder, there does appear to be a definite forward swing of the tufts as the trailing edge tip is approached, and some of the outer tufts near the leading edge look as if they are curving forward and inboard. The odd single tuft streaming aft at the trailing edge still appears, but its location moves inboard with increase in incidence; thus at 15° it is at 0.2 semi-span, and at 18° it is about 0.1 semi-span. At 0.56 semi-span at 18° one tuft can be seen to be spinning strongly, presumably indicating the presence of a shed vortex.

In order to detect the presence of the suspected laminar separation bubble vortex near the leading edge, tufts pivoted on pins projecting from the wing surface were located along the leading edge. External tufts were mounted on stings projecting from the wing under-surface. In Fig.18 it will be seen that at 8° all the tufts stream along the line-of-flight, with a well defined wing tip vortex. Increase to 10° causes the outermost leading edge tuft to swing round to lie parallel to the edge; the external tuft remains streaming almost normal to the pivoted tuft, showing that the free stream is still flowing parallel to the plane of symmetry of the wing.

At/

At 11° the spanwise flow along the leading edge is well established, as even the tuft at 0.56 semi-span is streaming spanwise. The tuft at 0.44 semi-span is inclined outwards, but it never swings round to become parallel to the leading edge. This suggested that somewhere in this region there was a divided flow in the boundary layer.

6.4 Liquid Film Studies*

Since tufting was obviously too coarse a method for detecting the highly localized vortex formations within the boundary layer, a technique which had been successfully used in early investigations of laminar-turbulent transition phenomena was applied. This was to spray the model with a suspension of lamp-black in paraffin with the wind off, and then immediately on completion of spraying, turn the wind on. The flow within the boundary layer was then clearly indicated by the movement of the liquid film, and regions of intense vorticity were located immediately by the rapid accumulation of lamp-black within them. A further advantage was that after a few minutes with the wind on the paraffin evaporated, leaving a flow pattern dried onto the wing surface which could be studied at leisure or photographed.

Sketches and photographs showing how the flow developed are shown in Fig.19.

The first evidence of the formation of a bubble vortex appeared at 6° incidence. The wing leading edge on the upper surface was scrubbed clean back to about 0.02 chord, and immediately behind the scrubbed area, a narrow band of lamp-black accumulated over a spanwise section of the inboard leading edge, and farther outboard from about 0.8 semi-span to the tip. Within the vortex, there was a strong spanwise flow which pulled the liquid towards the wing tip. The vortex followed the curve of the wing tip back to the trailing edge. The spanwise regions between the two vortices appeared to have normal laminar-turbulent transition on the surface.

At 8° the vortex extended the whole length of the leading edge, except near the root, where it curved aft before fading out. The band of lamp-black tapered, with its broadest width inboard, and approached the leading edge towards the tip. While the wind was on, and before the liquid dried, a thin column of liquid could be clearly seen flowing steadily right along the leading edge and accumulating in a small patch at the leading edge tip. This accumulated liquid remained stationary at this point and rotated clockwise, i.e., when looking at the upper surface of a port wing.

With further increase to 10°, the vortex band formed slightly nearer the leading edge and extended nearer to the root. At the tip, the small patch previously noted became more expansive, and trails of liquid round it indicated clockwise rotation over a larger region. The flow along the wing tip curve was now in two distinct parts; forward, it was towards the leading edge and aft it was towards the trailing edge. At mid semi-span, there were signs of a slightly unsteady rearward breaking of the spanwise band of liquid.

At 11° there was a marked change in the pattern. The bubble vortex appeared along the leading edge outboard from the root, but about mid semi-span, it swung aft abruptly and an intense band of liquid flowed steadily along it chordwise towards the trailing edge. Just outboard of this change of direction, the leading edge was scrubbed clean, but slightly farther outboard a new vortex, much narrower and closer to the leading edge, could be seen to grow.

The close-up view shows the vortex at the point where it swings aft. The faint lines in the photograph are 0.025 chord apart, so it will be seen that the bubble is about this width, but narrows to about 0.01 chord before it turns.

Just/

---

*A preliminary note describing the results of these liquid film studies has already been published (J.R.Ae.Soc., April, 1952). The greater part of that note is repeated here in order that the results may be more easily related to the earlier pressure measurements and tuft studies.

Just outboard, the smooth deposit of lamp-black suggests normal transition, and beyond this, the beginnings of a new vortex can be discerned. This is extremely narrow, appearing as a slightly darker thin line much closer to the leading edge than the main bubble vortex.

At the trailing edge, the chordwise vortex turned and fluid flowed along the edge out to the tip. Most unexpectedly, it did not collect there, but turned and flowed forwards in a narrow band towards the leading edge. It proceeded inwards along the leading edge to accumulate in a marked vortex with its axis normal to the surface at the junction with the outward flow along the leading edge. The main portion of the boundary layer between the chordwise vortex and the tip flowed outwards and then swung round, as sketched. In the photographs, this region always appears almost clear of lamp-black, because the scrubbing action of the flow seems to be very powerful, so that fluid is either swept aft to feed the flow along the trailing edge, or forward to feed the trail coming along the tip.

At 12° the pattern exhibits the same features, but the chordwise flow now starts farther inboard and towards the trailing edge the vortex curves outboard more to flow along it. Instead of flowing right to the tip, it starts swinging forward at about 0.9 semi-span, and similarly, instead of following the wing tip curve, it slopes more sharply inboard to meet the "standing" vortex on the leading edge. This has also moved farther inboard to about 0.8 semi-span.

With further increase of incidence, the features become more marked. The leading edge "standing vortex", which is now indicated by an approximately circular accumulation of liquid with a diameter of about 5% mean chord rotating very vigorously, moves closer and closer inboard until at 18° it is about 0.45 semi-span. The curvature of the flow from the trailing edge starts about mid semi-span, and has completely turned inboard within 0.8 semi-span. A column of liquid streams in from the extreme rear tip to feed this main stream and flows into the standing vortex. There is still a small bubble vortex parallel to the leading edge, but it extends only to about 0.2 semi-span before being swept round aft. Trails of fluid feeding into the main stream outboard of the standing vortex indicate clearly the nature of the flow surrounding it.

The under surface of the wing was sprayed and examined at various incidences, with particular attention to the leading edge region on the opposite side to the standing vortex. There was smooth laminar-turbulent transition on the surface, and no sign of the standing vortex. The vortex is thus confined to the upper surface.

This unexpected and most surprising behaviour of the flow in the boundary layer helps to explain some of the puzzling features of the earlier results. Thus in the spanwise distribution of pressure along the constant percentage chord lines (Fig.5) the suction peaks moving inboard with incidence, at the leading edge and x/c of 0.05, from the extreme tip at 9° to 0.83 semi-span at 12°, and to 0.44 semi-span at 18°, coincide exactly with the location of the standing vortex at these incidences.

The increase of the normal force curve slope for the inboard and outboard sections starting at 6° incidence, discussed in Section 4 (Fig.6), may now be assumed to arise from the fact that at this incidence a laminar separation bubble vortex forms parallel to the leading edge at these sections and so effectively provides a thicker aerofoil section which must have an increased slope associated with it. At 12° the vortex lies spanwise from the root to about 0.44 semi-span before swinging aft, and hence only the sections inboard of this location continue to benefit in this way. Conversely, at the same incidence the boundary layer flow over the tip region is towards the leading edge, and this causes the tip sections to stall.

With increase in incidence the inward movement of the standing vortex leaves, outboard of itself, a regime of flow which provokes stalling, and so the stall progresses inboard with increase in incidence, in all cases being initiated at the leading edge.

The location of the bubble vortex along the leading edge at low incidence and its subsequent meanderings over the wing surface can be related to the pressure gradients indicated in the isobar distributions (Fig.3), especially the flow into the standing vortex, which occurs at the region of highest suction on the wing. The pressure distributions do not help to explain the rearward swing of the bubble vortex, however, because from Fig.5 it will be seen that there is a favourable pressure gradient along the leading edge, 0.05 and 0.1 chord out to 0.8 semi-span at 12°, and 0.6 semi-span at 15°, yet the vortex swings aft about 0.46 and 0.4 semi-span respectively.

The/

The explanation may be that between 0.05 chord and the leading edge the pressure gradients differ in trend from those in Fig.5 and that detailed investigation would reveal a localized adverse gradient spanwise which would be sufficient to deflect the vortex rearwards. This is suggested by the fact that the phenomenon is critically dependent on the incidence, to the extent that a $\frac{1}{4}$ degree change either way will cause the vortex either to lie along the span or abruptly swing aft. When the incidence is altered to and fro, the spanwise flow can be made to bifurcate, responding very rapidly to the changing conditions.

The inability of the boundary layer yawmeter to give sensible readings at higher incidences (Section 6.2) is now easily explained. Rotation through $\pm 20^\circ$ would still not align the head anywhere near the flow, which is inboard towards the leading edge, whereas it had been preconceived to be flowing chordwise from the leading edge.

The effect of boundary layer fences, as fitted to some aircraft, has been studied*. In the light of the flow patterns shown above, the fences would not be expected to influence the stalling behaviour of the wing. A typical example with two nose fences extending two-thirds of the chord aft is shown. It will be seen that there are two strong "standing" vortices formed on the leading edge outboard of each fence, the main flow along the trailing edge appearing to divide to flow forward in both regions of the wing.

Inboard of each fence, there is formed a strong "standing" vortex. The growth of the "standing" vortex at the leading edge tip, and its subsequent movement inboards, is not affected by the presence of the fences.

7. Conclusions

7.1 The overall normal force coefficient $\bar{C}_n$ increased linearly with incidence over the range tested, 0° to 18°. The pitching moment curve, $\bar{C}_m/4$ against $\bar{C}_n$, was linear up to a $\bar{C}_n$ of about 0.5. At this point there was a small 'bump' in the curve, which was followed at a slightly higher $\bar{C}_n$, but still well below $\bar{C}_{n\,max}$, by a marked change in slope of the curve. Examination of numerous other results has shown that many sweptback wings tested have exhibited a similar 'bump' in their pitching moment curves at some moderate value of $\bar{C}_n$.

7.2 The $\bar{C}_n$ at which the 'bump' in the curve appears coincided with the onset of tip stalling, as indicated by pressure distribution measurements.

7.3 Investigation of the boundary layer with a liquid film technique has revealed the formation of a "bubble" vortex under the separated laminar boundary layer at the nose. This first appeared at 6° incidence and grew spanwise with increase of incidence to 10°. There was a strong spanwise flow within the "bubble" region.

At 11° the "bubble" vortex swung aft abruptly about mid semi-span, and a new phenomenon, a "standing" vortex with a core normal to the wing surface, became well established at the tip. This "standing" vortex moved inboard with further increase in incidence.

The growth and inward movement of this vortex appears to be closely associated with the stalling behaviour of the wing and requires further investigation. It does seem, however, that the combination of the abrupt rearward change of direction of the "bubble" vortex, and growth in strength of the "standing" vortex, coincides with the 'bump' in the pitching moment curve.

While the Reynolds number of this test was admittedly comparatively low, it is believed that the phenomena described will exist at higher Reynolds numbers, since they originate with laminar separation, which is relatively independent of Reynolds number.

8. Acknowledgements

The author wishes to thank Prof. A. R. Collar for his advice and criticism throughout the course of the investigation. He is also indebted to the Editor of the Journal of the Royal Aeronautical Society for permission to reprint Fig.19 and for assistance in its reproduction for this report.

9./

*The full results of this fence investigation are to be published.

9. List of References

No.	Author(s)	Title, etc.
1	G. G. Brebner	Pressure and boundary layer measurements on a 59° sweptback wing at low speed and comparison with high speed results on a 45° swept wing. Part II. A.R.C. C.P.86, 1952.
2	G. B. McCullough and D. E. Gault	Boundary-layer and stalling characteristics of the NACA 64A006 airfoil section. N.A.C.A. Technical Note No.1923. (August, 1949).
3	J. Weber	Low speed measurements of the pressure distribution near the tips of sweptback wings at no lift. R.A.E. Report No. Aero.2318. (March, 1949). A.R.C. 12,421
4	A. W. Babister	Measurements of the pressure distribution on swept back wings with trailing edge split flaps. Summary of wind tunnel work at the College of Aeronautics 1948-50. College of Aeronautics Report No.43. (March, 1951). A.R.C. 14,009
5	D. Küchemann, J. Weber and G. G. Brebner	Low speed tests on wings of 45° sweep. Part II. Balance and pressure measurements on wings of different aspect ratios. R. & M. 2882. May, 1951.
6	R. E. Dannenberg	Measurements of section characteristics of a 45° swept wing spanning a rectangular low-speed wind tunnel as affected by tunnel walls. N.A.C.A. Tech. Note No.2160. August, 1950.
7	B. H. Wick	Chordwise and spanwise loadings measured at low speed on a triangular wing. N.A.C.A. Tech. Note No.1650. June, 1948.
8	J. Weissinger	Lift distribution of sweptback wings. Forshungsbericht Nr.1 JJ3 (February, 1942). Trans. in N.A.C.A. T.M. No.1120.
9	R. Stanton-Jones	An empirical method for rapidly estimating the loading distributions on sweptback wings. College of Aeronautics Report No.32. (January, 1950). A.R.C. 12,997
10	F. W. Diederich	A simple approximate method for obtaining spanwise lift distributions over swept wings. N.A.C.A. RM L7107, May, 1948.
11	E. J. Hopkins	Lift, pitching moment, and span load characteristics of wings at low speed as affected by variations of sweep and aspect ratio. N.A.C.A. Tech. Note No.2284, January, 1951.
12	N. H. van Dorn and J. DeYoung	A comparison of three theoretical methods of calculating span load distribution on swept wings. N.A.C.A. Tech. Note No.1476, November, 1947.
13	J. DeYoung	Theoretical additional span loading characteristics of wings with arbitrary sweep, aspect ratio, and taper ratio. N.A.C.A. Tech. Note No.1491, December, 1947.

TABLE 1/

TABLE 1

Aerofoil Section Ordinates

Dist. from L.E. % c	Semi-ht. of Section % c
1.0	1.10
2.5	1.73
5.0	2.42
7.5	2.89
10.0	3.30
15	3.90
20	4.32
25	4.63
30	4.84
35	4.97
40	5.00
50	4.83
60	4.31
70	3.48
80	2.42
90	1.22
100	0

TABLE 2

Position of Pressure Holes

	Hole No.	x % c
Upper Surface	1	L.E.
	2	5
	3	10
	4	20
	5	30
	6	40
	7	50
	8	60
	9	70
	10	80
	11	87.5
	12	95
	13	T.E.
Lower Surface	14	7.5
	15	15.0
	16	25
	17	35
	18	45
	19	55
	20	65
	21	75
	22	85
	23	92.5

JW

FIG. 1.

Mean Aerodynamic Chord = 10·7″
Aspect Ratio = 4·3
Taper Ratio = 0·326
L E Sweepback = 44°
¼c Line Sweepback = 40°

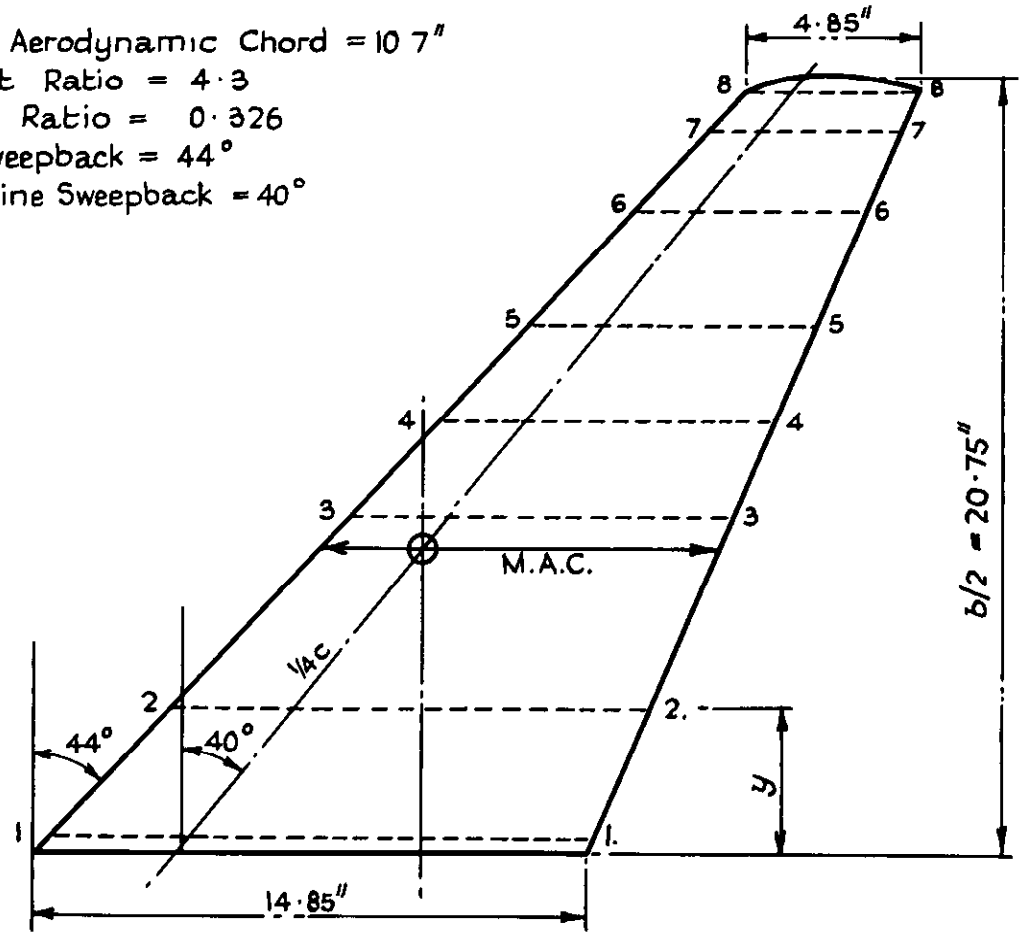

Chord	1	2	3	4	5	6	7	8
Span Position y/b/2	0·02	0·2	0·44	0·56	0·68	0·83	0·93	0·97

Aerofoil Section: 10% thick at 40% c.

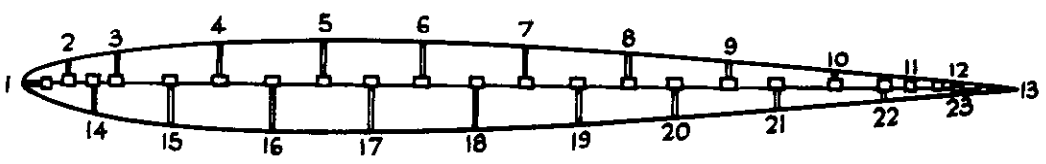

Details of Wing and Pressure Holes.

FIG 2

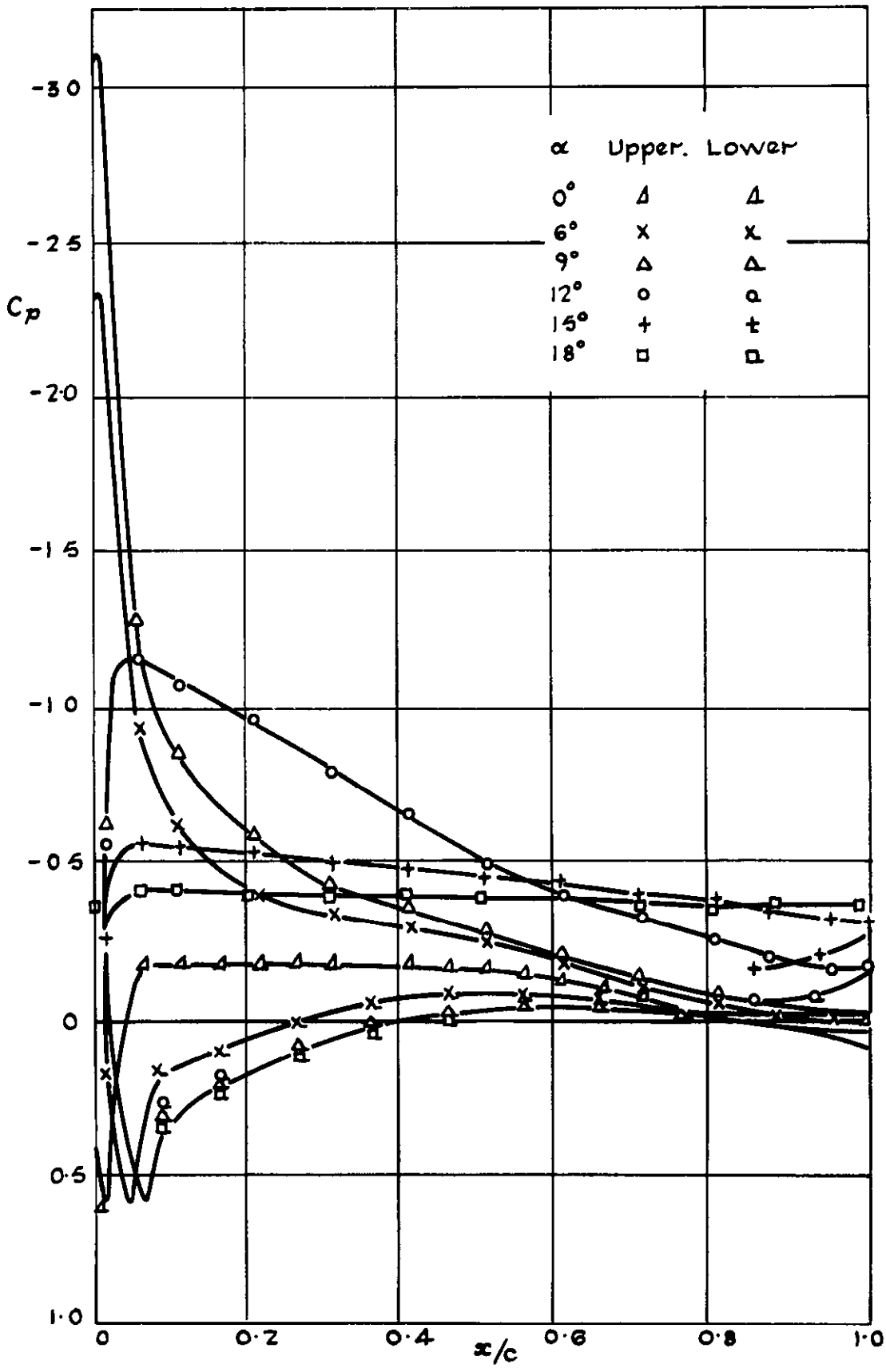

Chordwise Pressure Distribution at Various Incidences.
Span location $\frac{y}{b/2} = 0.83$

FIG. 3a

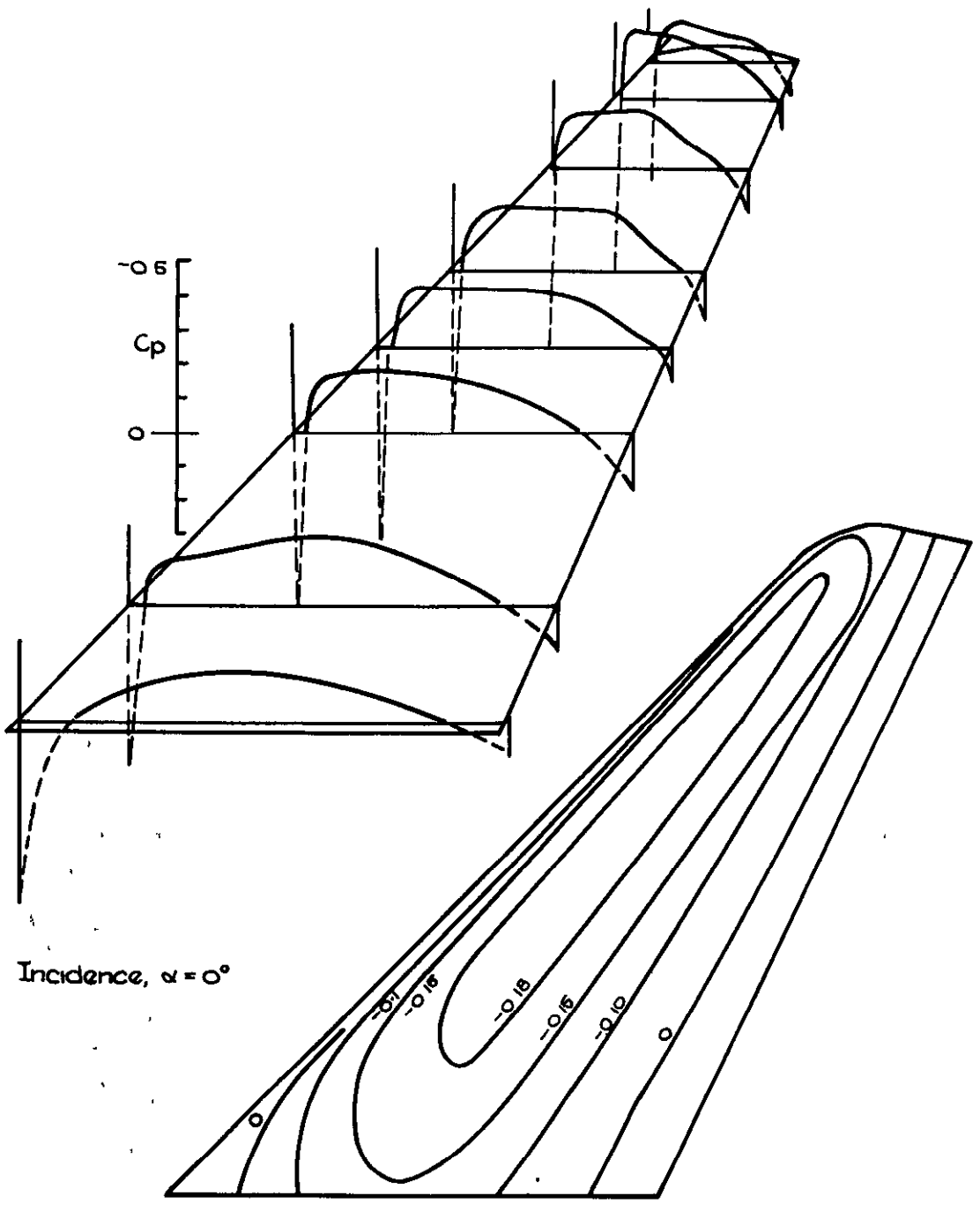

Chordwise Pressure Distribution Diagrams and Contours

Upper Surface

FIG 3(b)

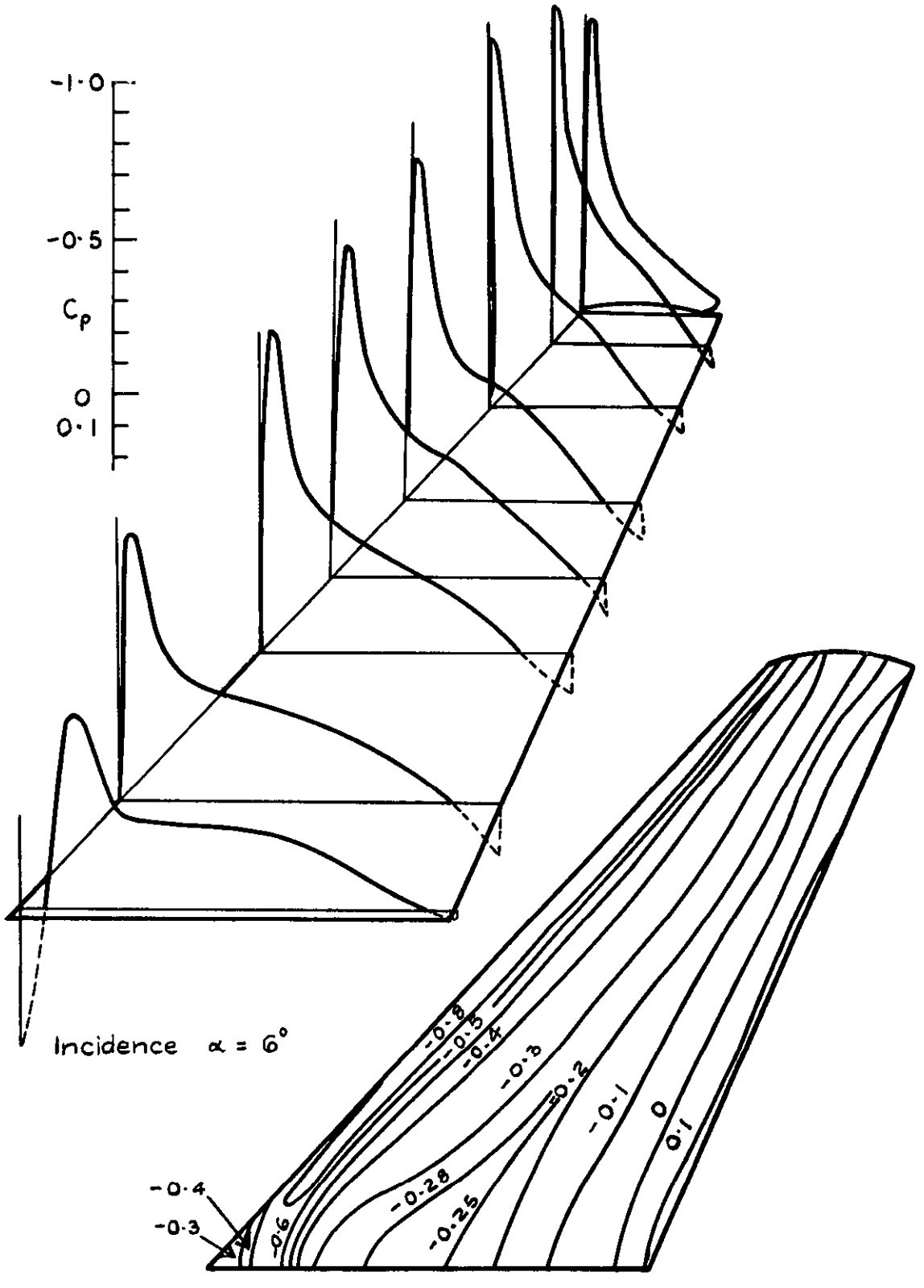
-1·0
-0·5
C_p
0
0·1
Incidence $\alpha = 6°$
-0·8
-0·5
-0·4
-0·3
-0·2
-0·1
0
0·1
-0·4
-0·3
0·6
-0·28
-0·25

FIG 3(c)

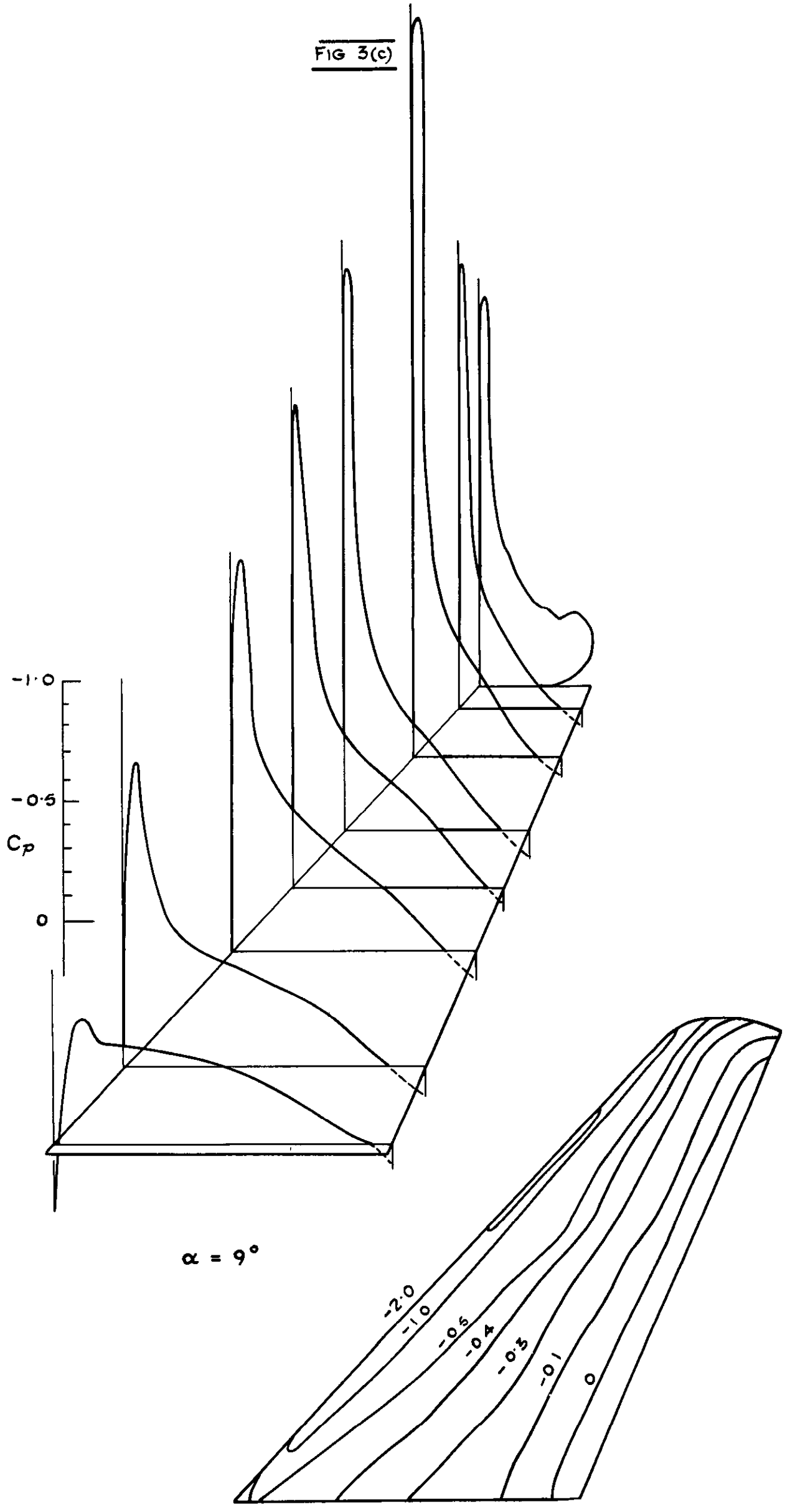

FIG 3(d)

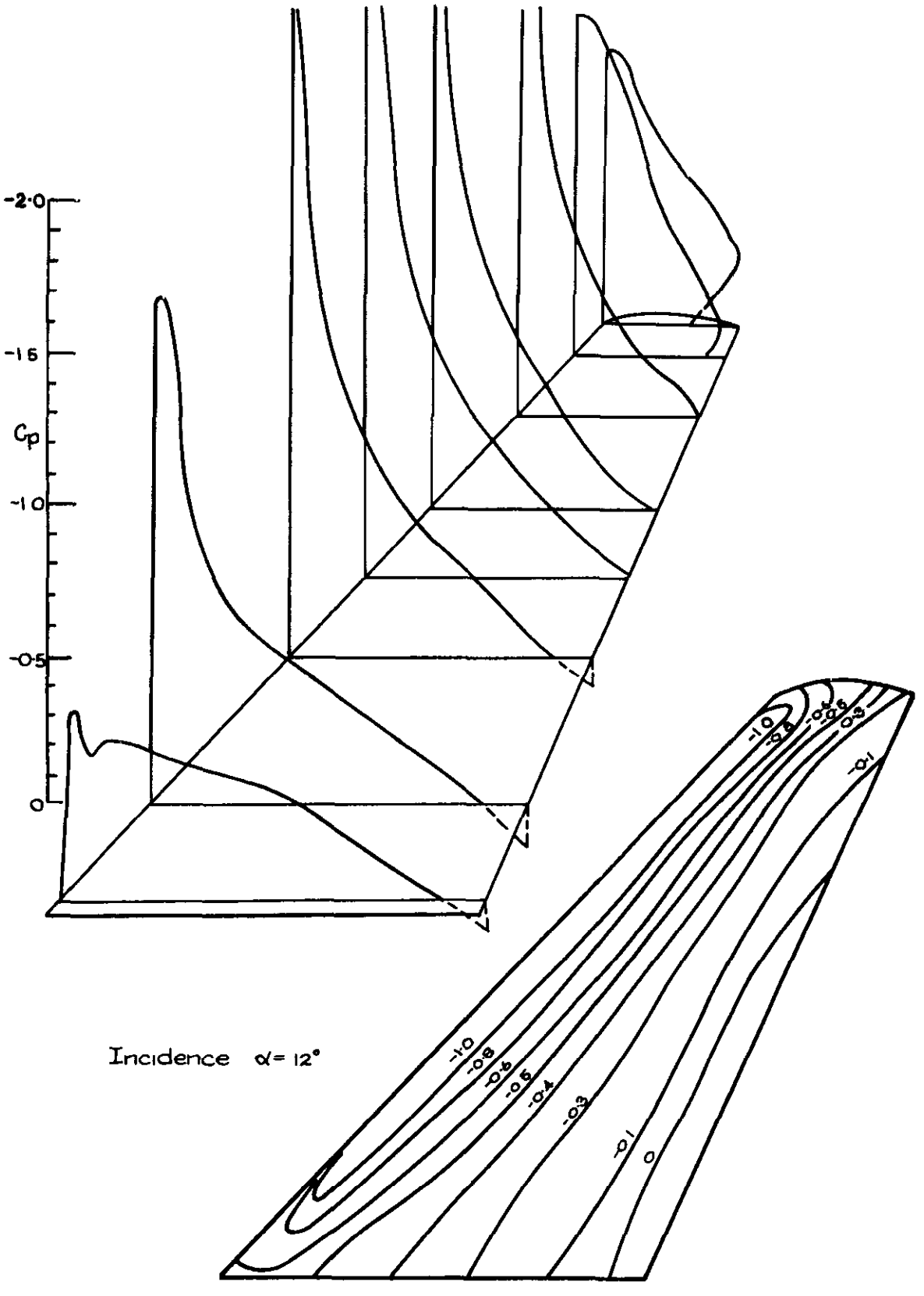

Incidence $\alpha = 12°$

Fig. 3(e)

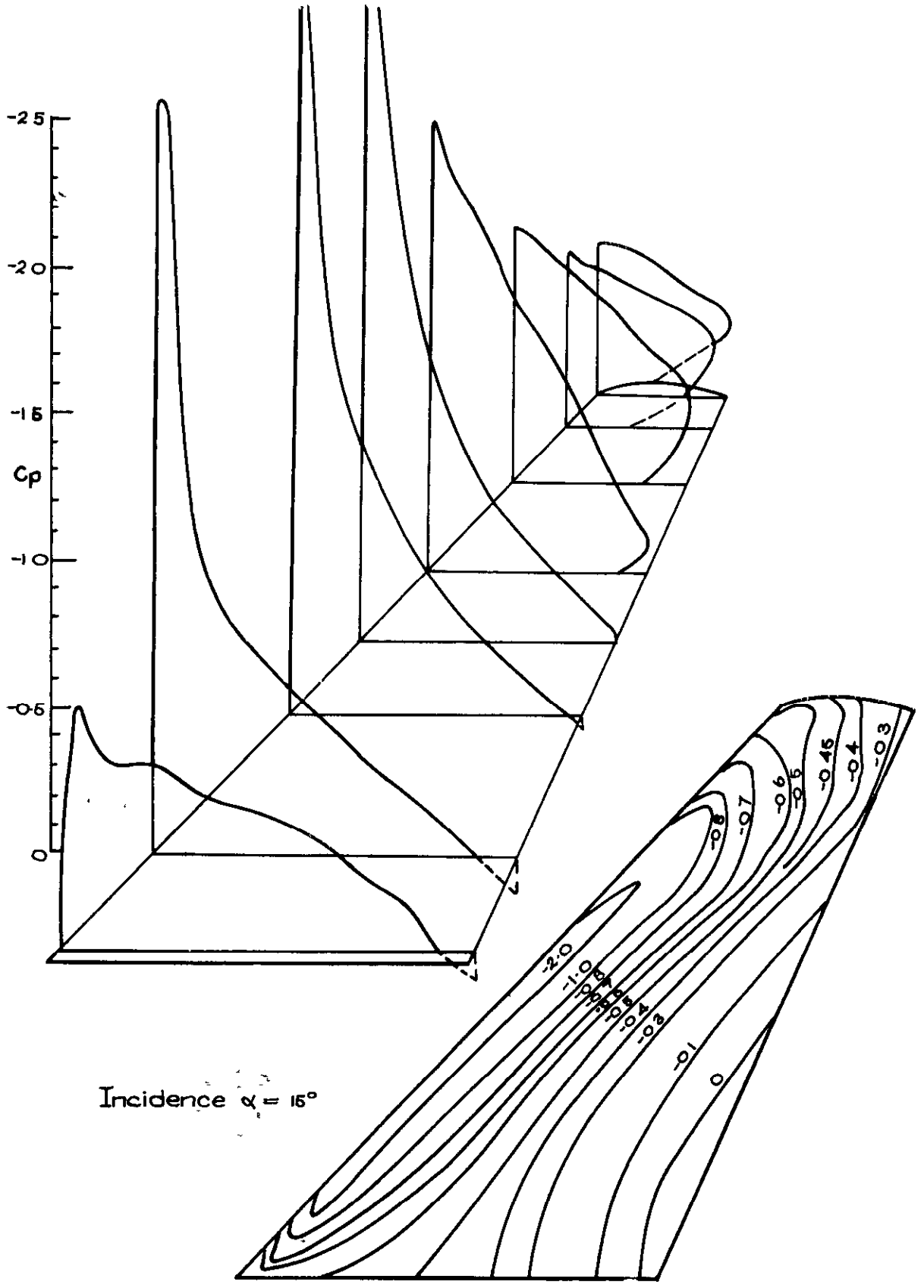

Incidence $\alpha = 15°$

FIG 3(f)

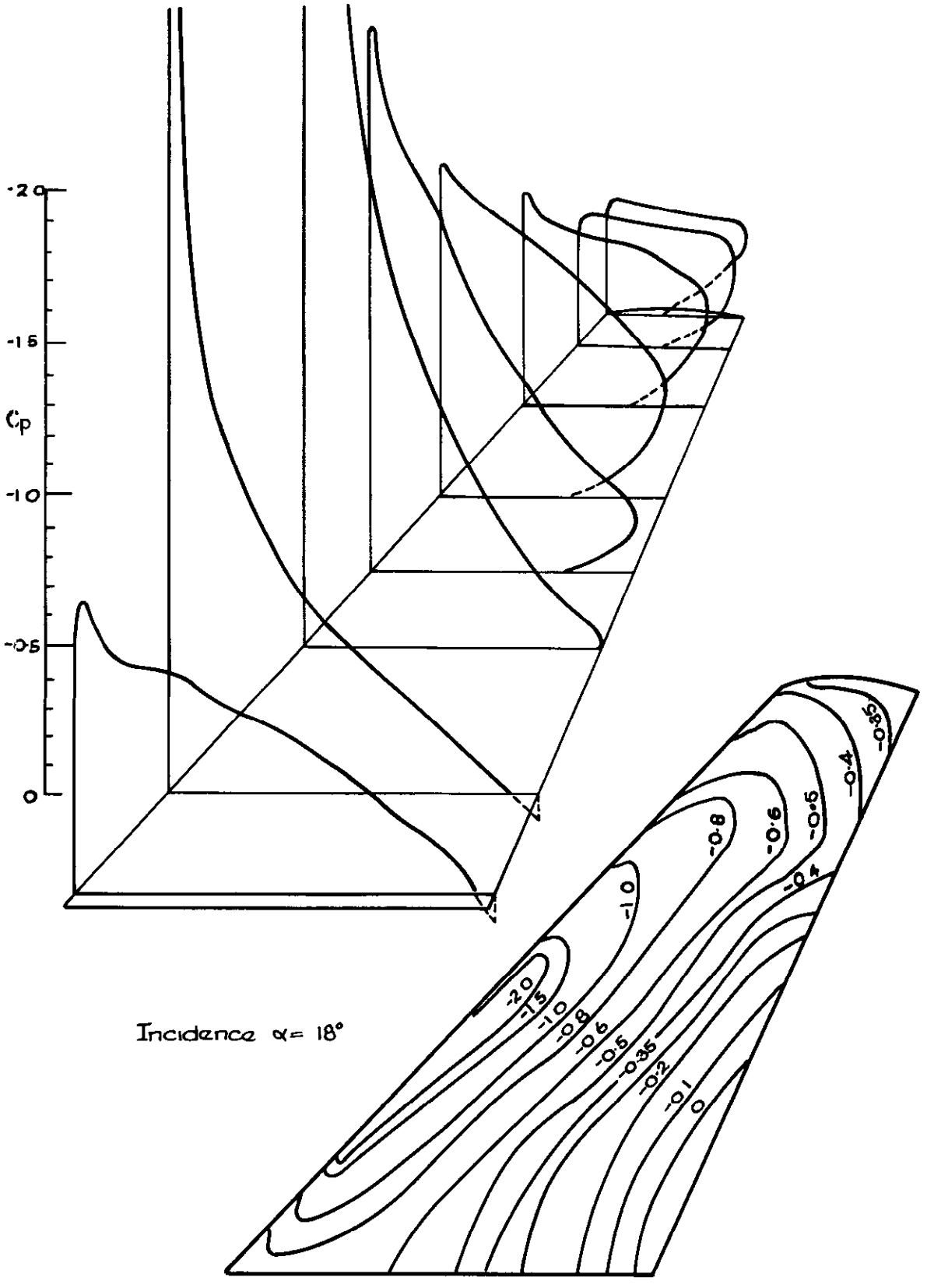

Incidence $\alpha = 18°$

FIG 4

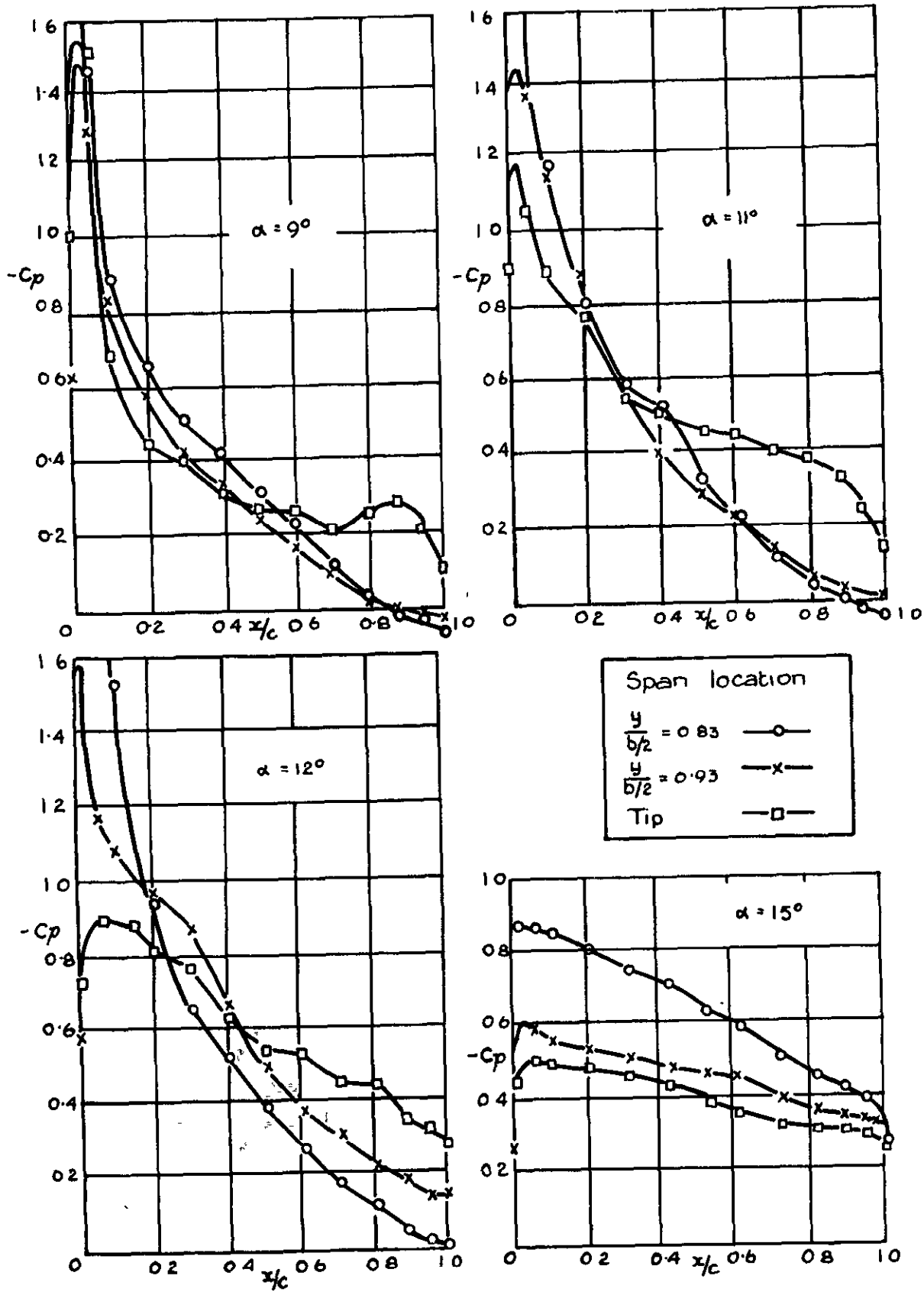

Chordwise Upper Surface Pressure Distributions over Tip Region

FIG. 5.

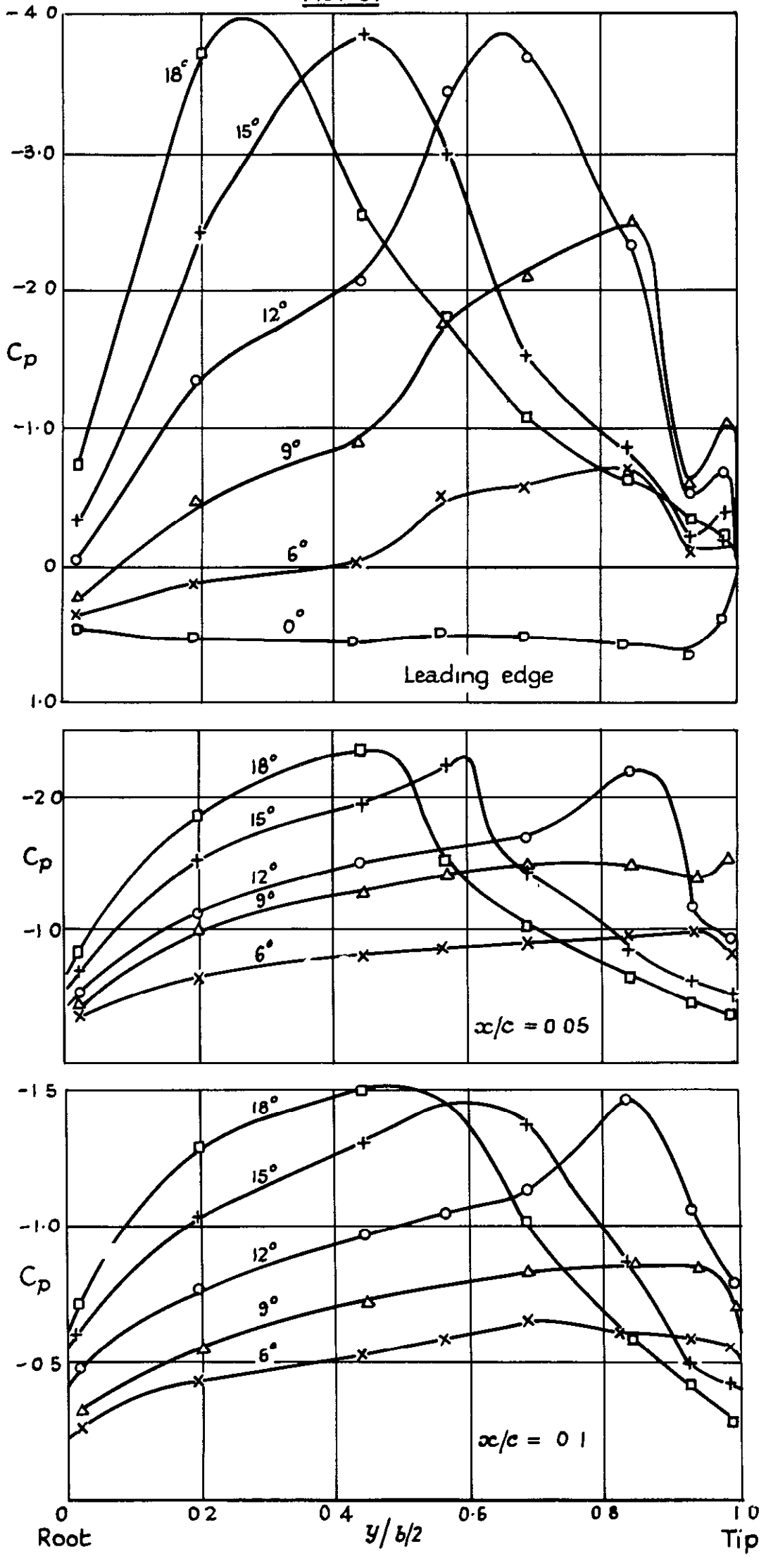

Spanwise Pressure Distribution along Constant Percentage Chord Lines, at Various Incidences (Upper Surface).

FIG 6

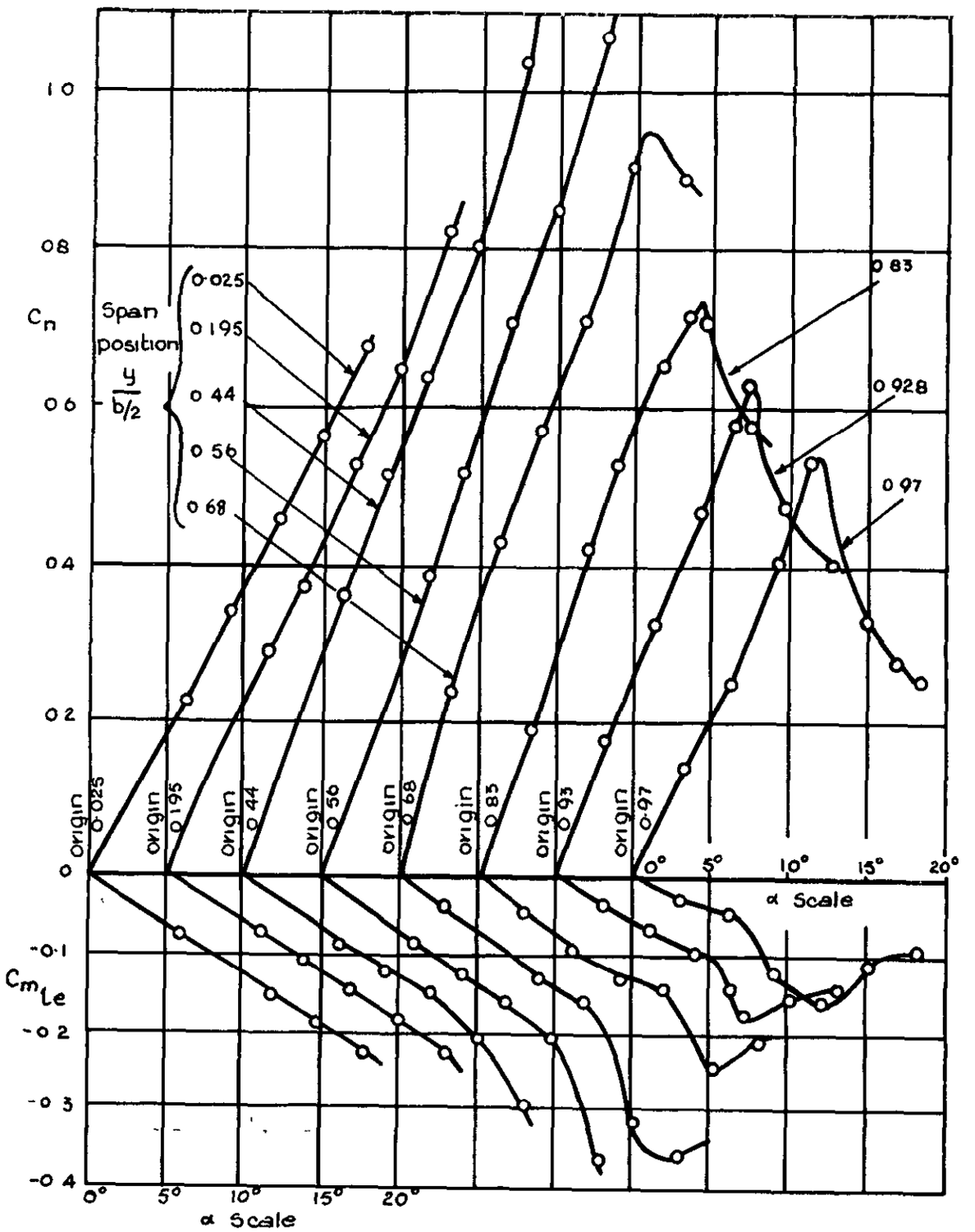

Section Normal-Force and Pitching Moment Curves along the Span

FIG 7.

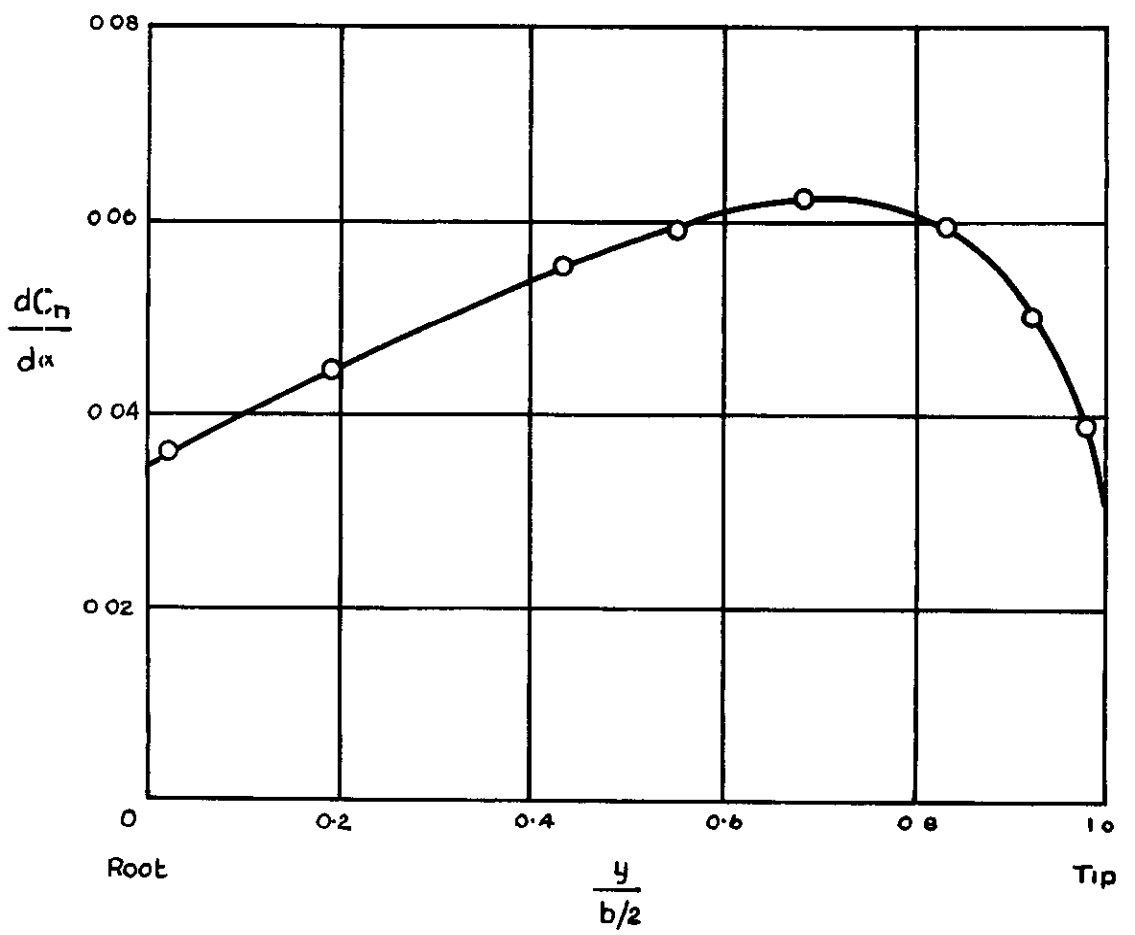

Spanwise Variation of Normal-Force Curve Slope

FIG. 8.

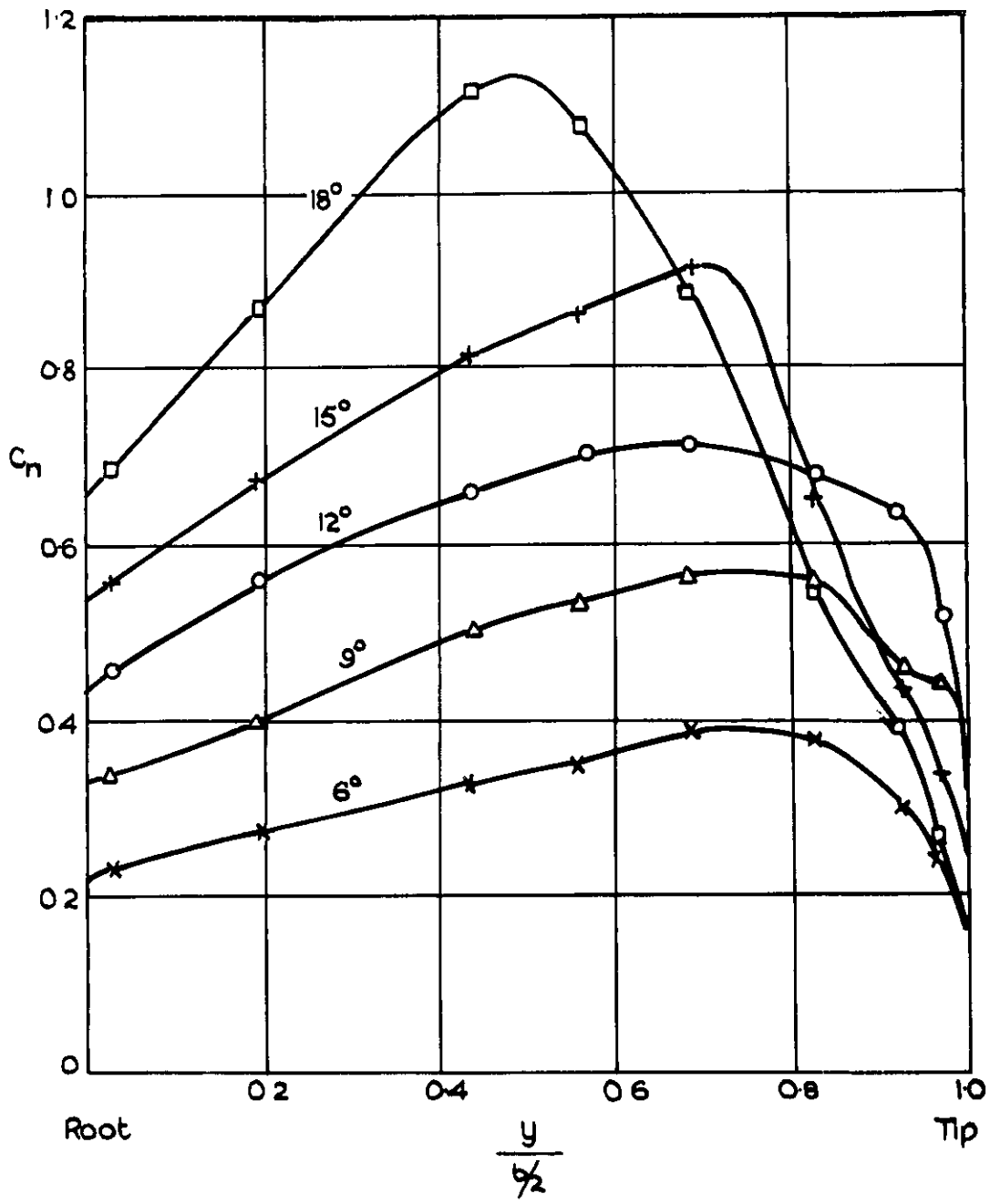

Spanwise Distribution of Section Normal - Force Coefficient at Various Incidences.

FIG 9

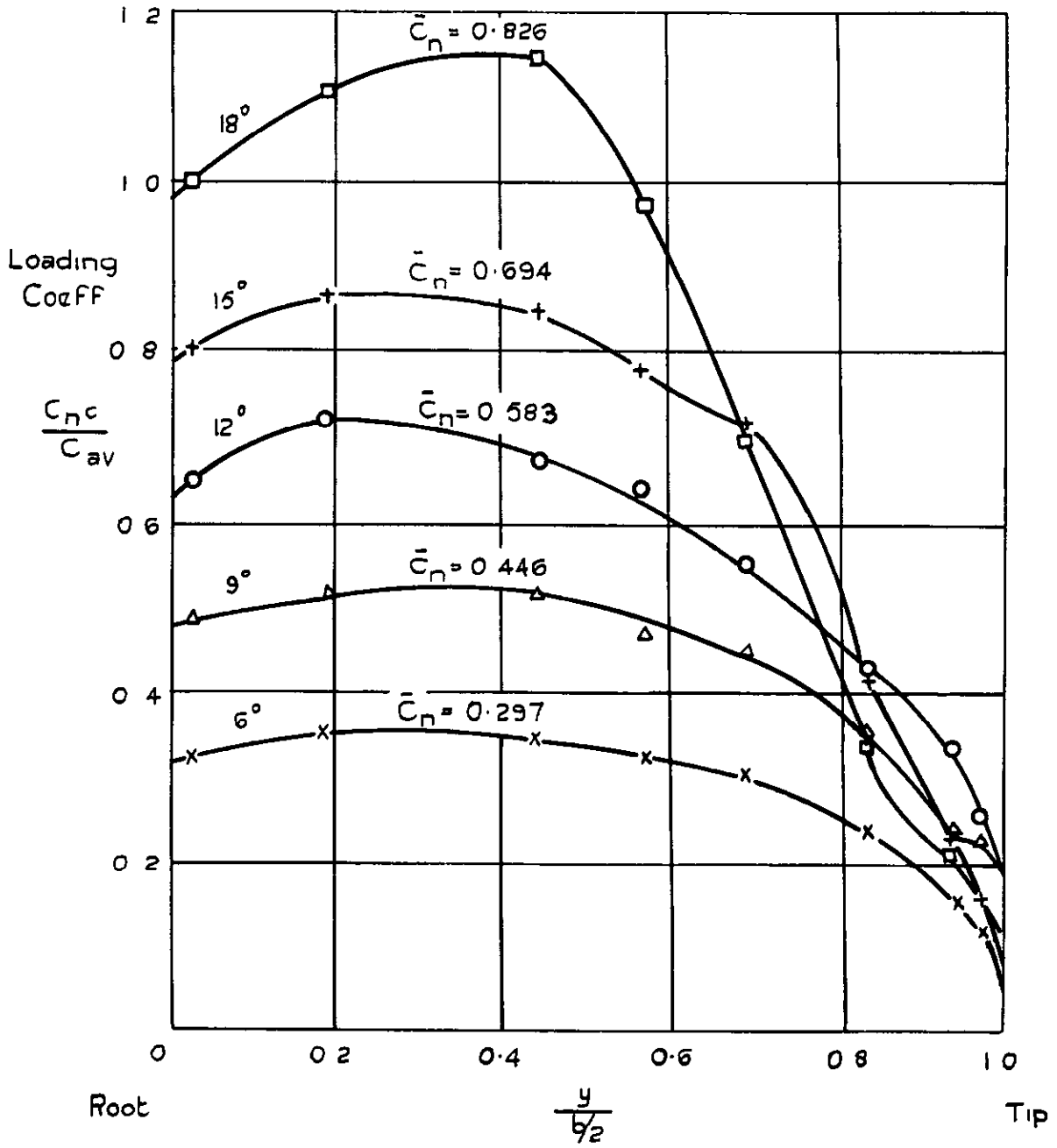

Spanwise Distribution of Loading Coefficient

Fig. 10.

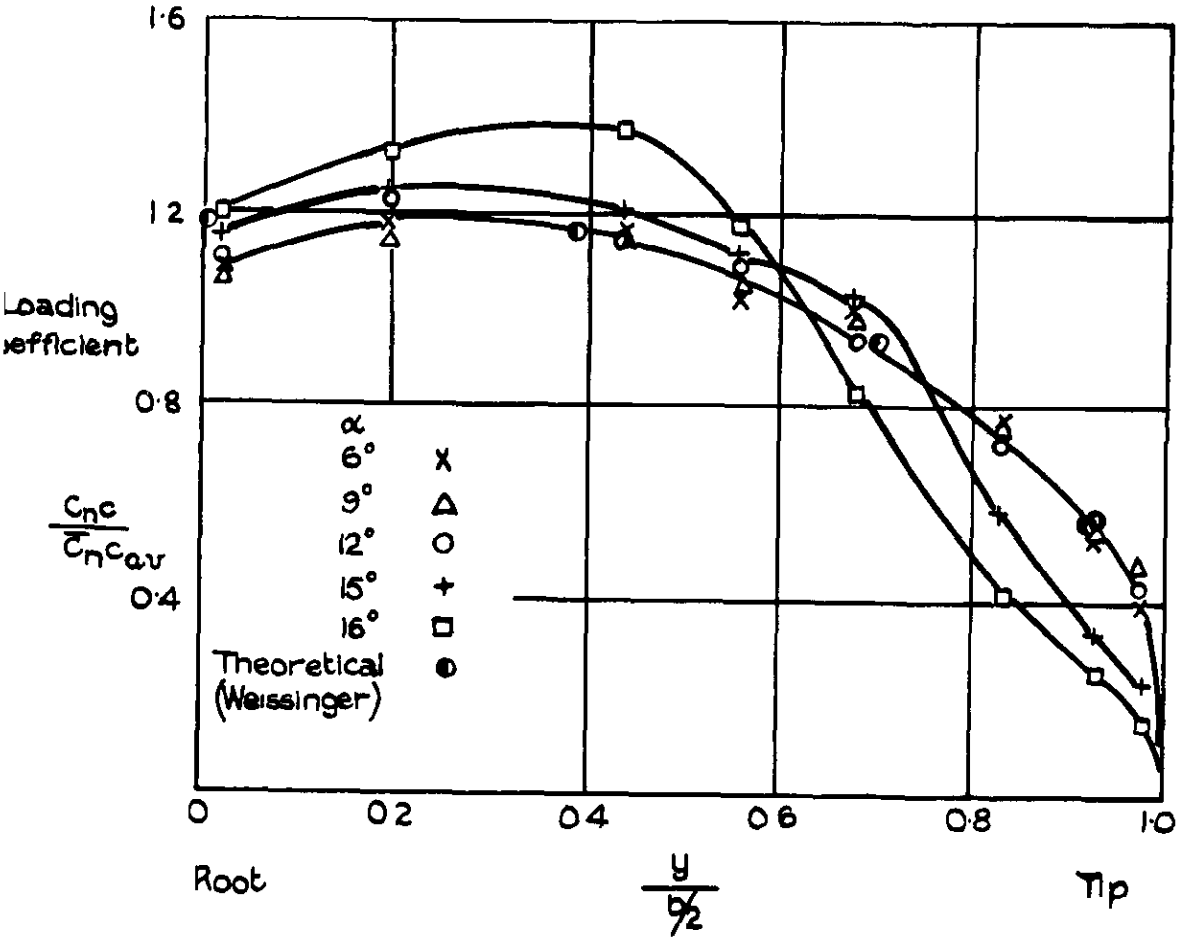

Spanwise Distribution of Loading Coefficient.

FIGS 11, 12 & 13

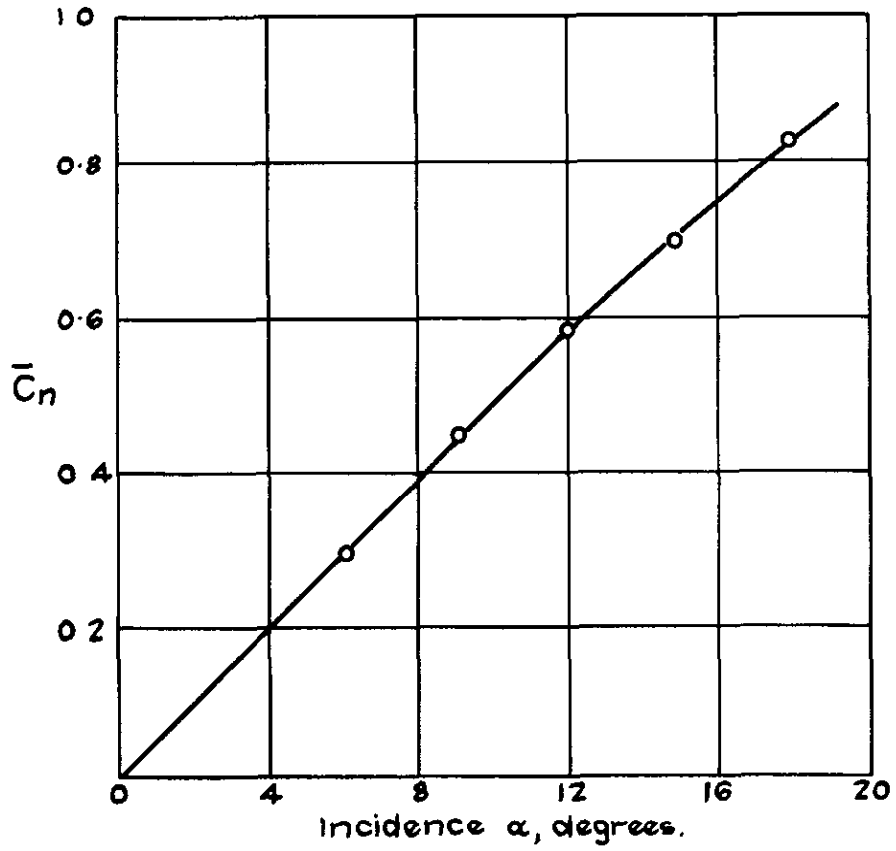

FIG. 11

Variation of Overall Normal-Force Coefficient with Incidence.

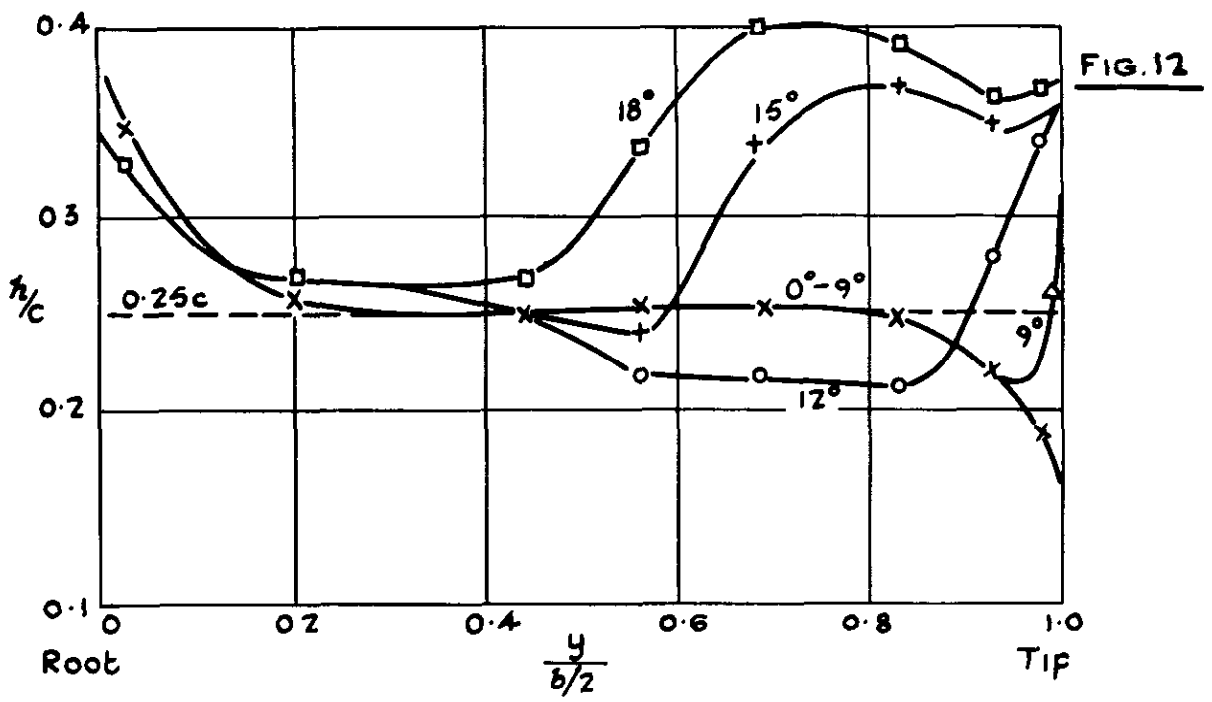

FIG. 12

Chordwise Location of Centre-of-Pressure along the Span.

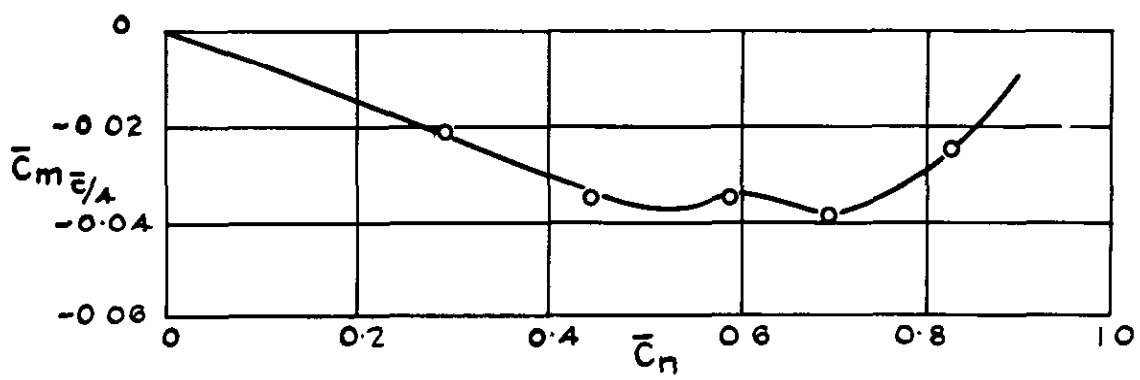

FIG. 13.

Variation of Overall Pitching Moment Coefficient about Mean Quarter-Chord with Overall Normal-Force Coefficient

FIG. 14

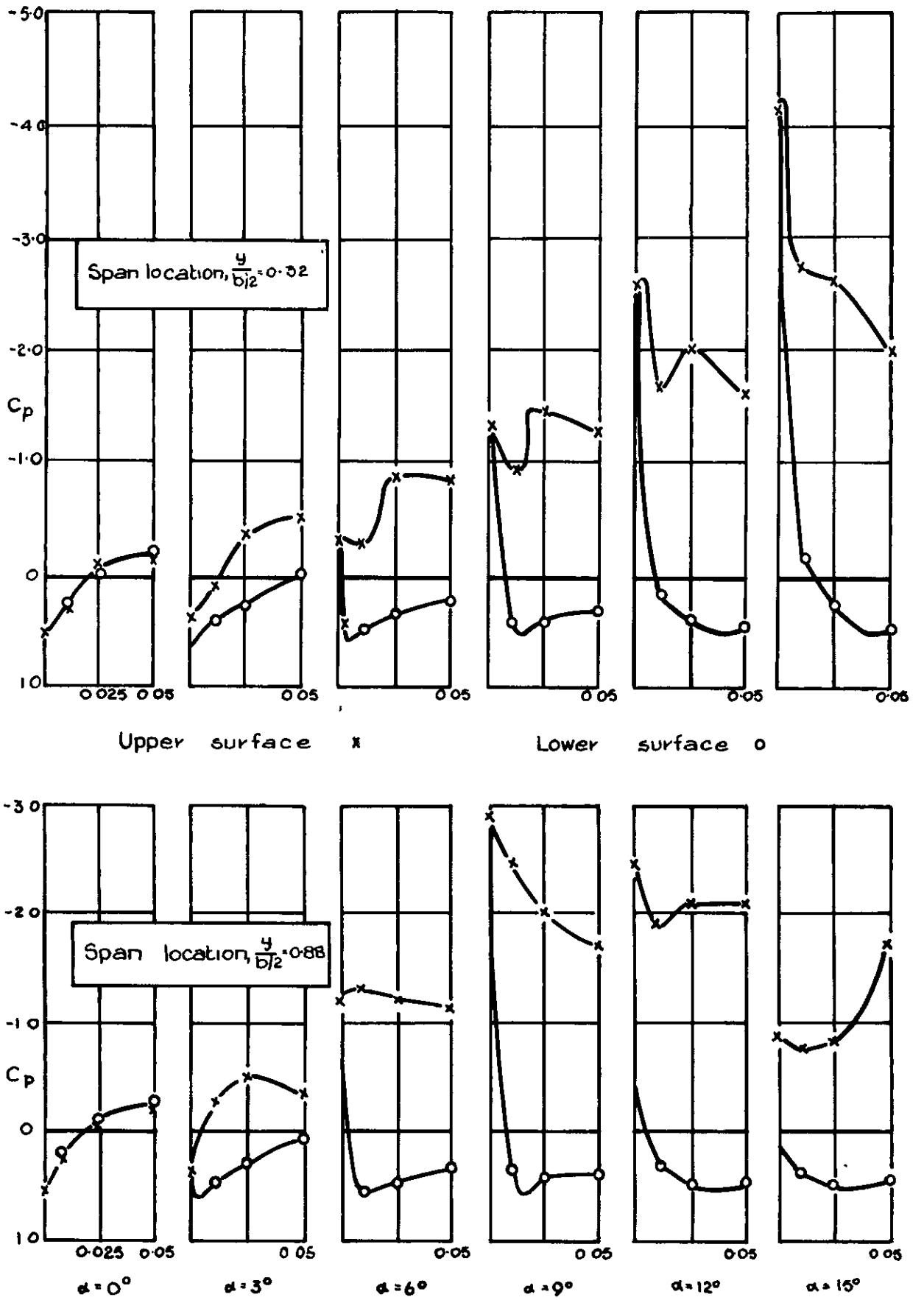

Pressure Measurements Round Section Nose at Two Spanwise Positions

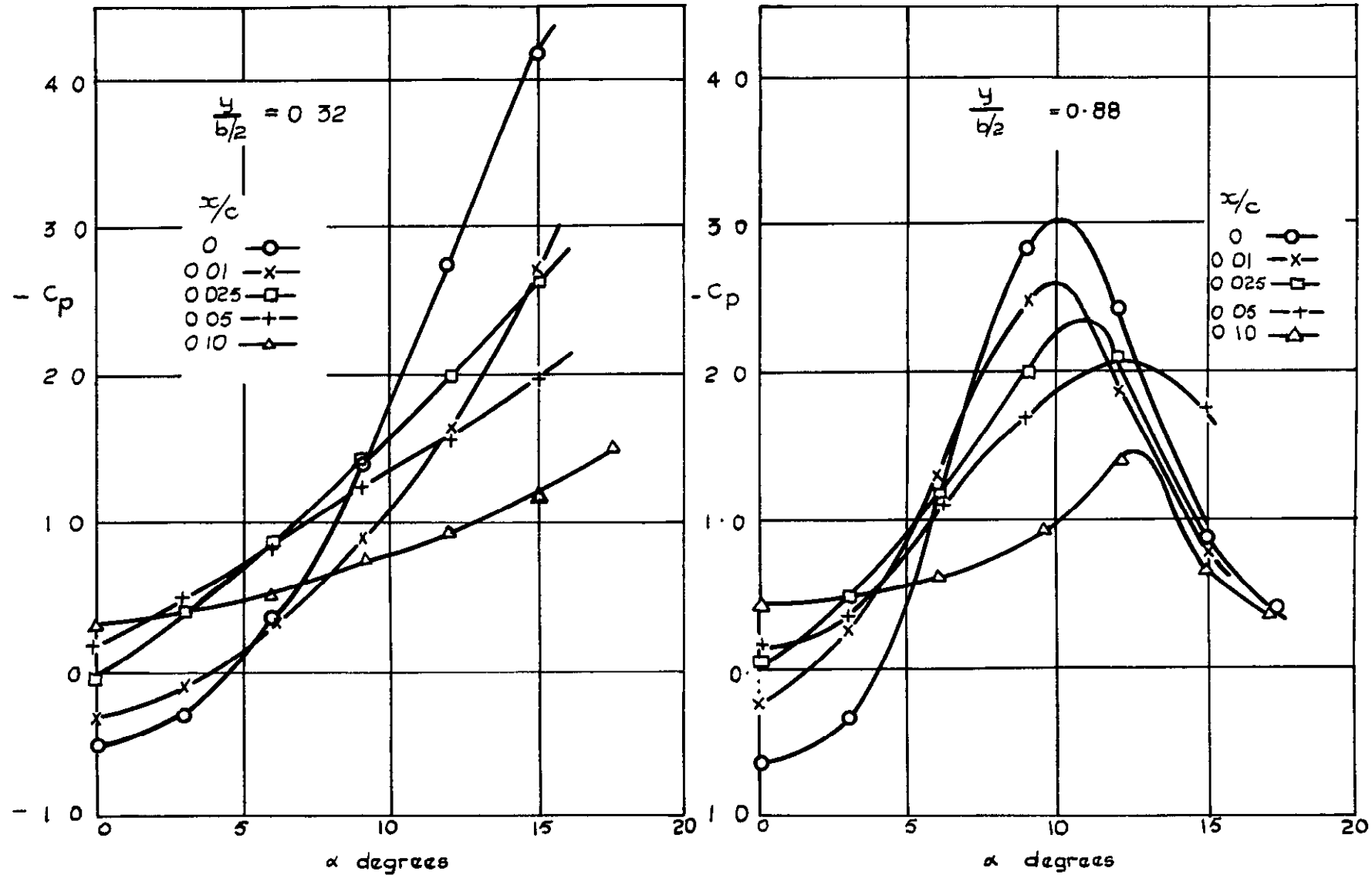

Variation of Upper-Surface Pressure with Incidence at Constant Chord Points, at Two Spanwise Locations

FIG 15

FIG 16

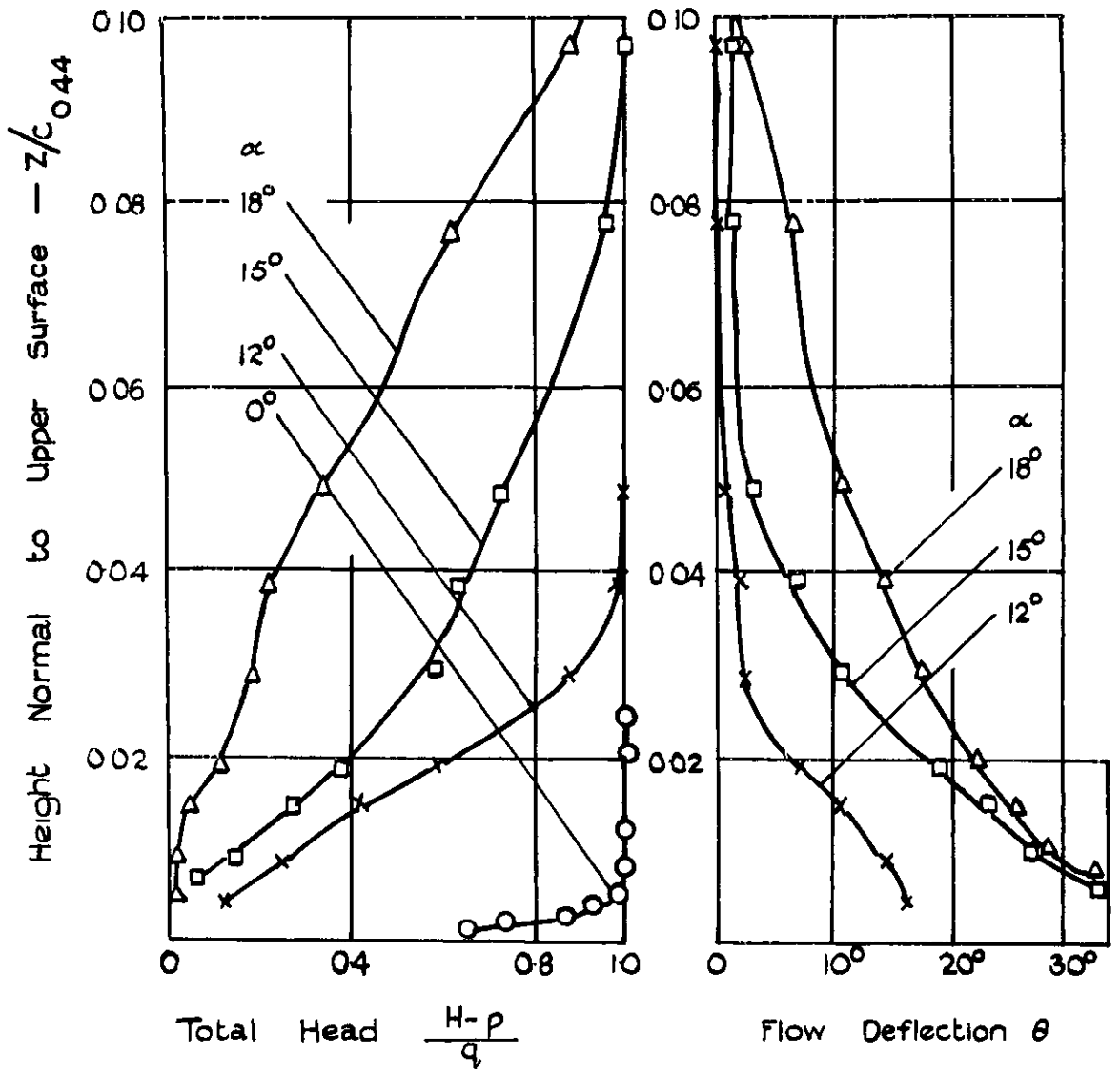

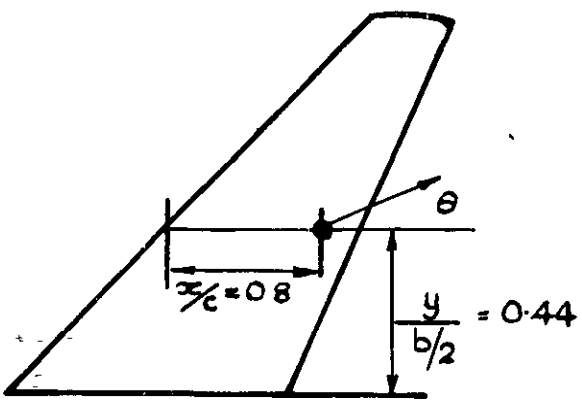

Boundary Layer Measurements at the Location Shown

0°

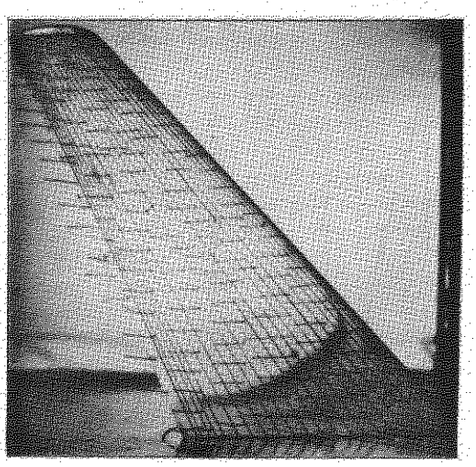

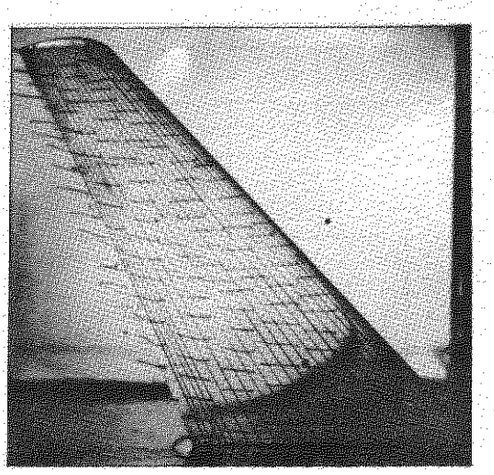

6°

9°

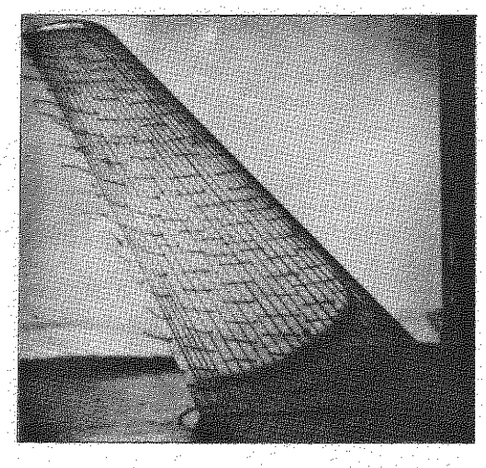

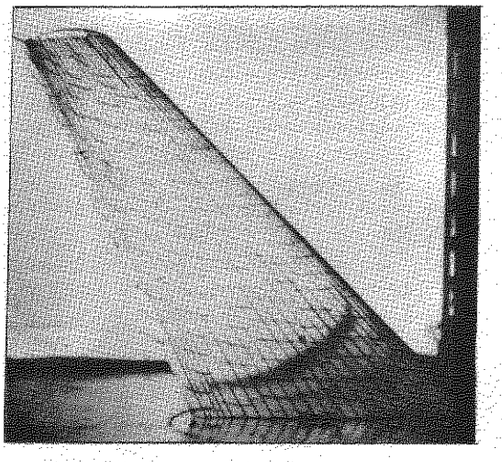

12°

15°

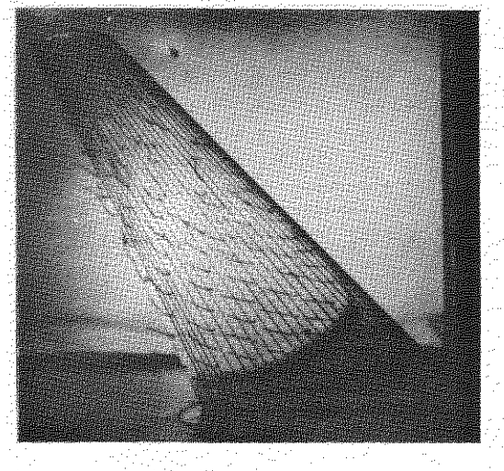

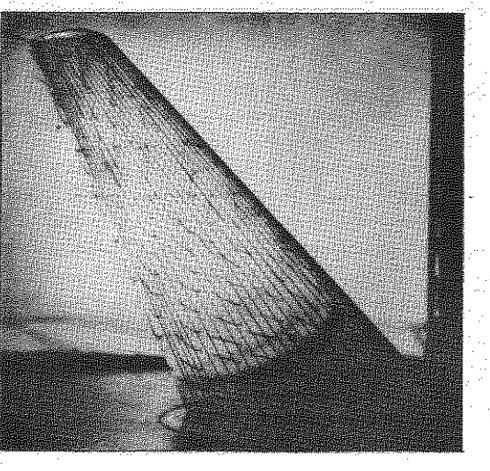

18°

Effect of Incidence on Tuft Behaviour.

FIG 18

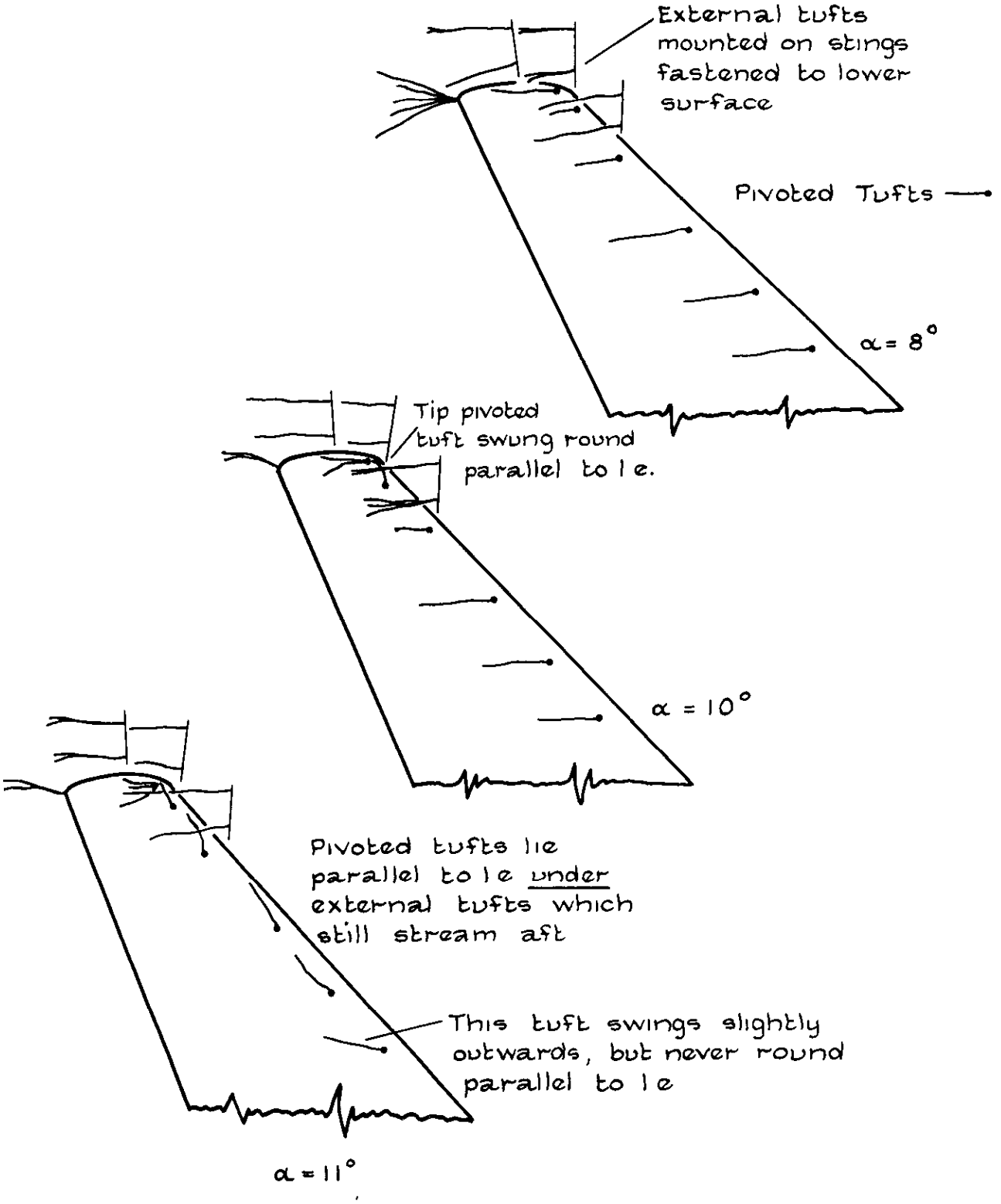

Behaviour of Pivoted Tufts along Leading Edge

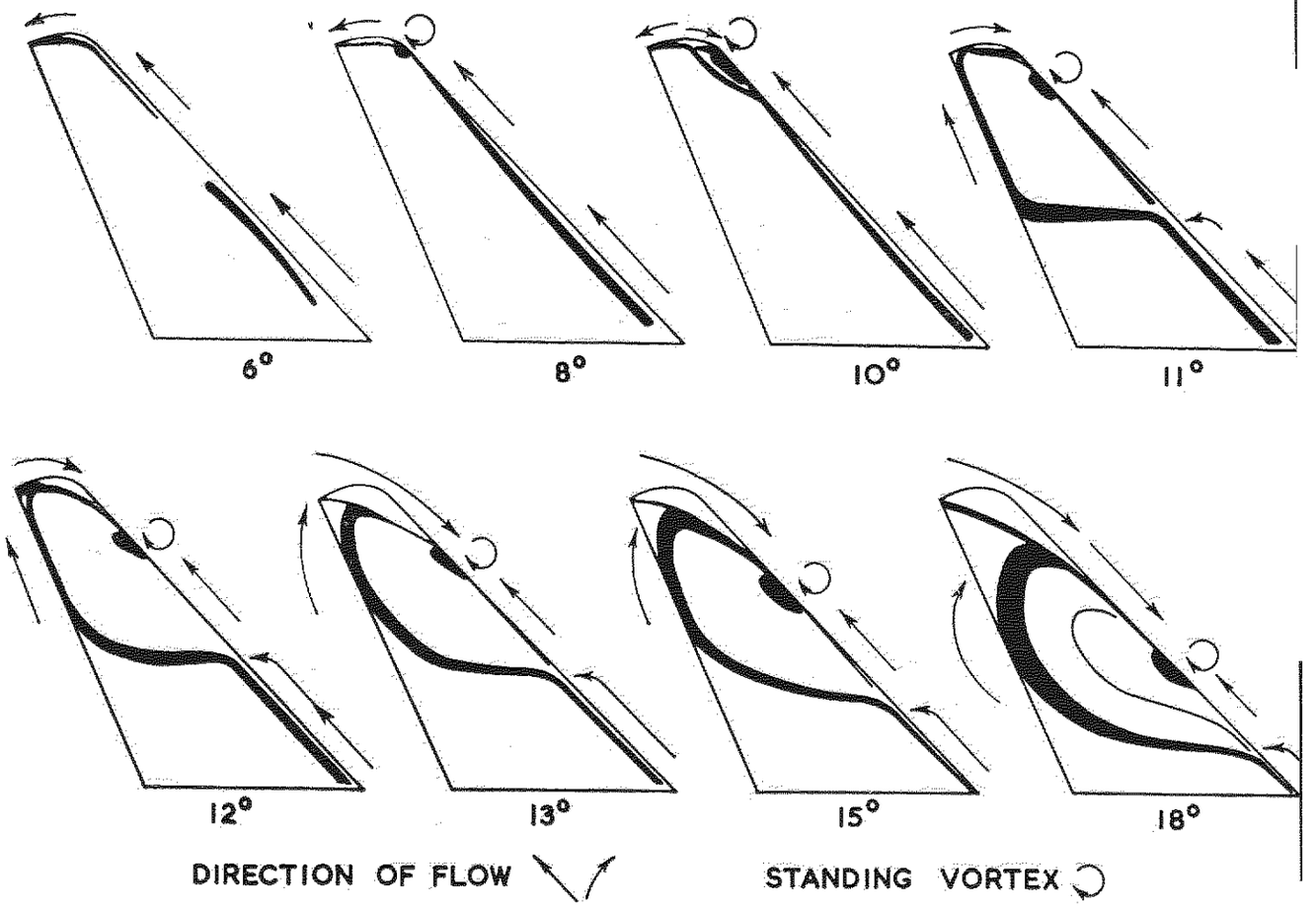

Fig. 1. Boundary layer lamp-black patterns.

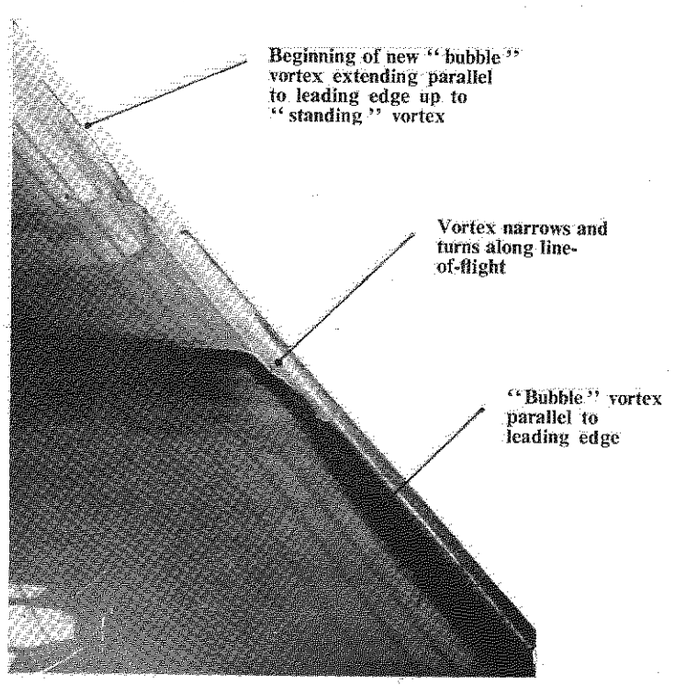

Fig. 3. Close-up view of separation "bubble" vortex where it turns along the line-of-flight direction.

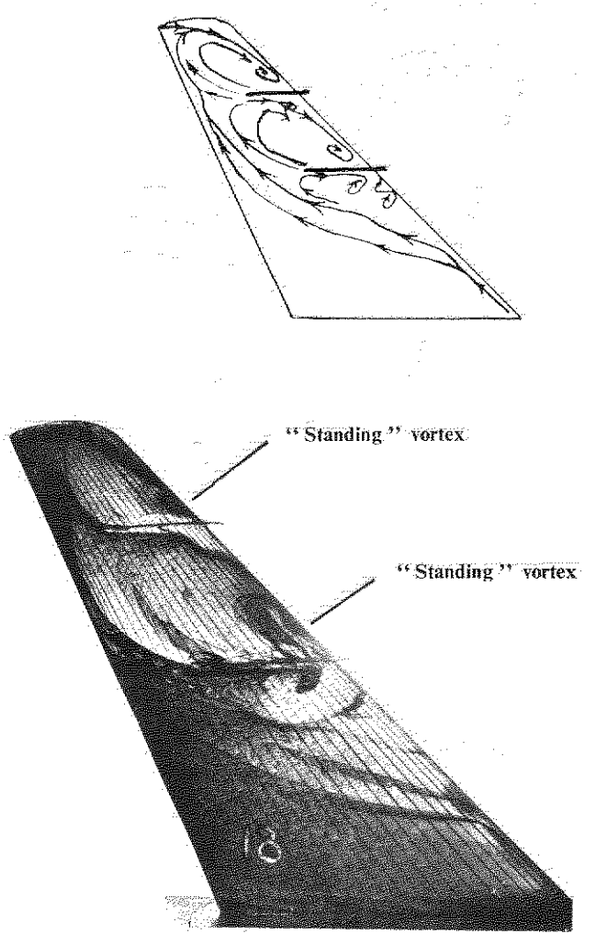

Fig. 4. Boundary layer pattern with two $\frac{2}{3}$ chord nose fences fitted. $\alpha=18°$.

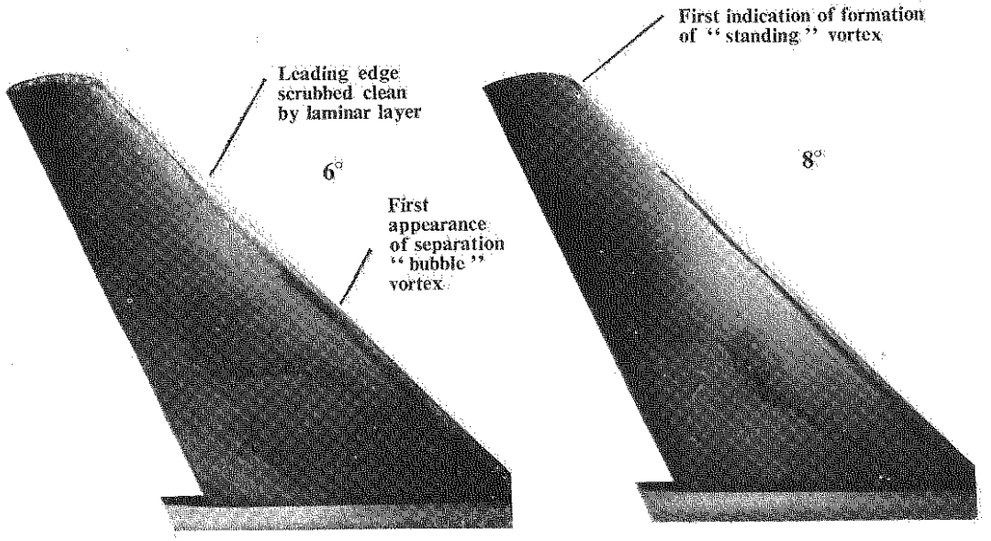

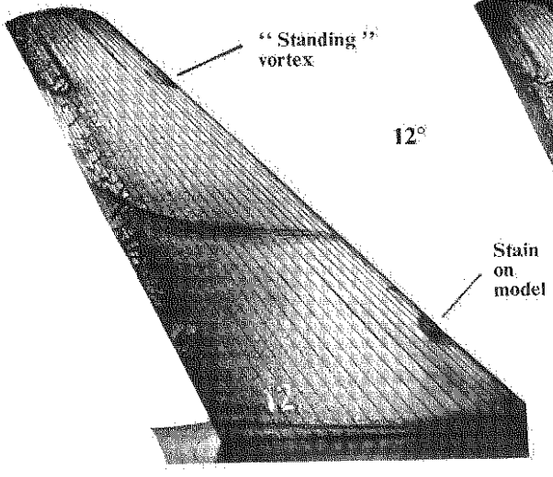

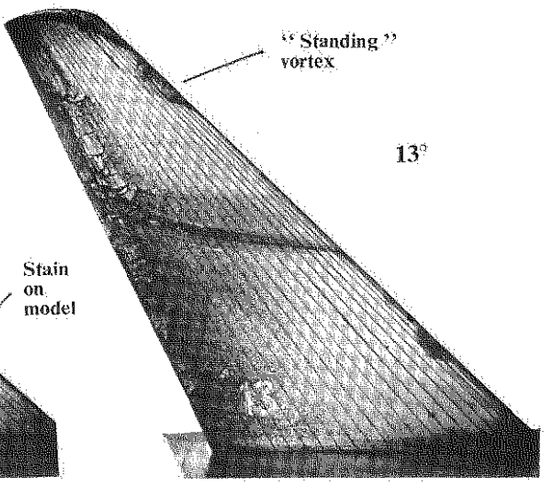

Fig. 2. Boundary layer lamp-black patterns.

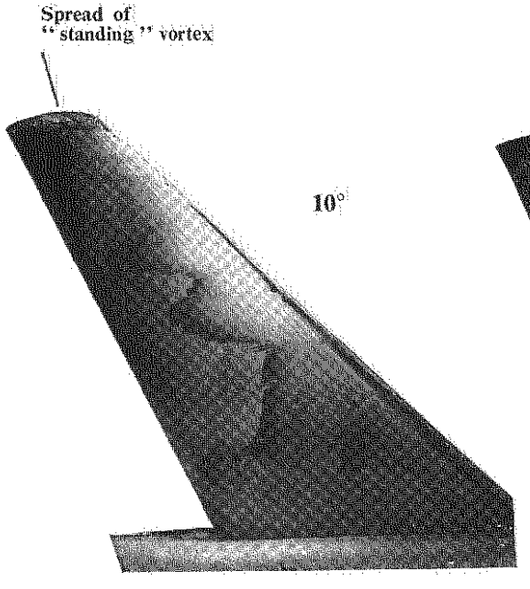

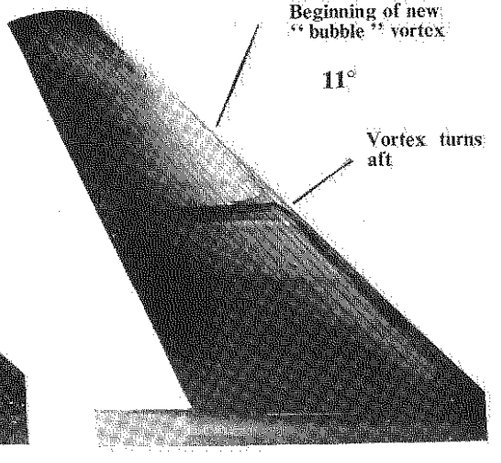

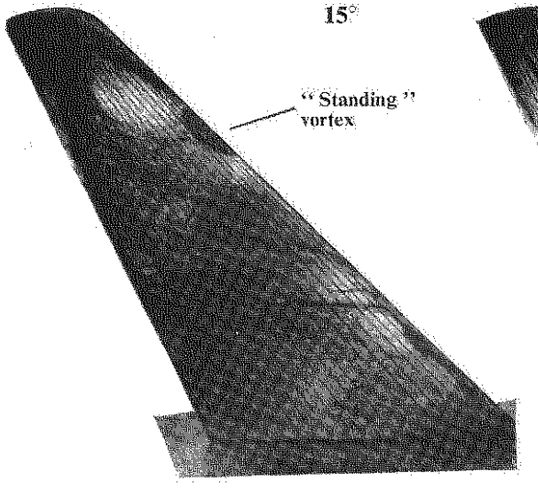

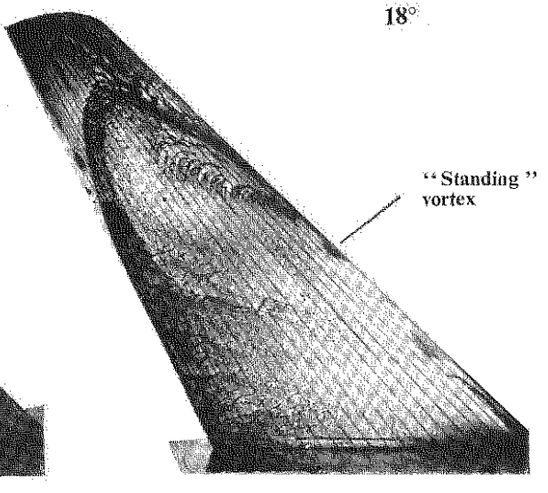

Fig. 2. Boundary layer lamp-black patterns.

FIG. 19

Addendum to Part II

August, 1953

Relation to Three-Dimensional Tests (Sect. 4.1.)

In this section of the paper the appearance of a localised constant-pressure region in the pressure distributions obtained in the two-dimensional tests was related to the change of direction of flow of the accumulated liquid near the leading edge of the three-dimensional wing, since both occurred at nominal incidences of between 10° and 11°. The incidences in the two tests bear no relation to each other, however, because of the "non-two-dimensional" character of the flow in the sectional tests; it is more correct to relate the phenomena on the basis of local normal-force coefficient, c_n. Thus in the sectional test the "short-separation" bubble was formed at a c_n of about 0.65 (Figs. 2 and 4, Part 2), and from Fig. 6 of Part I it will be seen that this value of c_n is reached at 0.56 semi-span at an incidence of between 10° and 11°. The change of direction of the liquid flow on the wing was observed about mid semi-span at this incidence, which suggests that the spanwise station where the liquid flow turns aft marks the inboard limit of the "short" separation bubble on the wing.

Part II

Two-dimensional Pressure Distribution Tests on a 10% Thick Symmetrical Aerofoil Section.

5th January, 1953

SUMMARY

Pressure distribution measurements, and liquid-film investigations of the boundary layer, have been carried out on a 10% thick, small nose radius aerofoil section at a Reynolds number of 0.5×10^6. The existence of a bubble vortex under the separated laminar boundary layer in the vicinity of the nose has been confirmed at incidences up to 10°.

Above this incidence, up to 15°, a different type of leading edge separation appears to take place, which closely resembles that occurring on a sharp-edged aerofoil. The flow separates immediately at the edge itself, and re-attaches further aft, with a bubble vortex located right on the leading edge. Failure of the separated flow to re-attach to the surface results in a collapse of the leading edge suction peaks, and produces an almost flat pressure distribution. Stalling of the section is thus accompanied by an abrupt decrease in lift just after $C_{L_{max}}$.

Similar results have been obtained in N.A.C.A. tests on various thin aerofoil sections at a Reynolds number of about 6 million, which suggest that up to this Reynolds number at least the main phenomena arising from separation of the flow in the vicinity of the leading edge are little influenced by Reynolds number, although the actual extent of the bubble vortex may be affected. Stream turbulence may possibly have some effect on the separation and subsequent vortex formation.

---

1. Introduction

Tests on the sweptback wing described in Part I of this report revealed the existence of a "bubble" vortex under the separated laminar boundary layer near the leading edge. Since the characteristics of the wing sections must be strongly influenced by the three-dimensional nature of the flow about the wing, it was difficult to assess whether the unexpected behaviour of the boundary layer was predominantly an inherent feature of the aerofoil section, or could be ascribed largely to the effects of sweepback. There is a considerable amount of information available about the formation of laminar separation vortices on some N.A.C.A. aerofoil sections[1-4], but it was felt that the two-dimensional characteristics of the actual section of the wing tested could be more closely related to the results obtained on the wing. Pressure distributions have therefore been measured on a new two-dimensional wing of the same aerofoil section as the original swept wing model.

2./

2. Description of Model, and the Tests

The section is 10% thick at 40% chord, with an elliptic profile from leading edge to maximum thickness; the nose radius was 0.007 chord. From maximum thickness to the trailing edge the profile is a quintic curve, with a 14° trailing edge angle.

A constant-chord wing, of chord equal to the mean aerodynamic chord of the tested wing, that is 10.7 inches, and span 6 inches, was constructed of Perspex; thirty pressure holes, distributed as shown in Fig. 1 were located along the chord (Table 1). The model was mounted between two large platforms, to ensure two-dimensional flow. It was found later that these platforms did not, in fact, simulate infinite aspect ratio; since the actual aspect ratio of the model was so small, and the effect of the platforms was unknown, no correction to the angles of incidence has been attempted here. All incidences quoted are therefore the actual settings of the model, relative to the free stream. The platforms did, however, prevent any spanwise flow, and thus the flow over the central region of the model was effectively two-dimensional, in contrast to that over the sections of the swept wing model.

Pressure distributions were measured over an incidence range from -6° to 20° at a wind-speed of 103 ft per sec corresponding to a Reynolds number of 0.57×10^6. In addition, liquid film studies of conditions in the boundary layer were made, using the lampblack-in-paraffin technique described in Part I.

3. Results

3.1 Pressure Distributions

Some of the measured pressure distributions are shown in Fig. 2. The suction starts to peak over the nose at 4° incidence, and a small constant pressure region is located about 0.2 of the chord at this incidence. With increase of incidence there is a rapid growth in the suction peaks over the leading edge, until at 10° a C_p of -3.0 is reached. Just aft of this suction peak a narrow constant pressure region is indicated. At 15° the maximum negative pressure measured, a C_p of -7.0, was found at the leading edge. An increase to 16° led to the collapse of this peak, and a wide constant pressure region formed aft of the leading edge with a pressure coefficient of just under -2.0; the leading edge hole still gave a peak reading of -3.0.

At 18° the stall was well established, but the leading edge still had a marked negative peak, followed by a slight dip. Further aft there was an increased suction over the section. An almost flat pressure distribution exists at 20°, but here again a highly localized suction persists right at the leading edge.

The development of the unusual pressure distributions over the leading edge of the section may be seen more clearly in Fig. 3, which is a large-scale plotting over the leading sixth of the chord. Up to 8° incidence the distribution has the usual smooth rise and fall of suction, but at 9° a slight inflexion of the curve occurs right at the leading edge. At 10° there is a marked change in the form of the distribution, with a constant pressure region from about 0.005 to 0.02 of the chord. With further increase in incidence, the suction right at the leading edge grows, and the distributions maintain a reflex curvature located about 0.02c right up to 15°.

3.2 Liquid Film Studies

The model was sprayed with a suspension of lampblack in paraffin, and the wind was then turned on rapidly. The first evidence of laminar separation appeared at 6°, when the leading edge was scrubbed clean, and a large quantity of lampblack accumulated in a band parallel to the leading edge from about 0.02 to 0.04 chord. The region of accumulation is indicated in Fig. 3 by shading.

The procedure was repeated at increasing incidences, but up to 10° there was no apparent change in the chordwise location or extent of the "bubble" vortex under the separated laminar layer. The turbulent layer aft of the "bubble" vortex appeared

to/

to be attached right to the trailing edge. At 11° the liquid film indicated some critical change in flow; a narrow band of lampblack accumulated as before about 0.025c, and in addition an intense and much narrower filament of fluid was located almost on the leading edge itself. Between the two bands of accumulated lampblack, the aerofoil surface was quite clean.

With further increase of incidence, the rear band of lampblack disappeared, and only the leading edge accumulation remained. This was extremely narrow, and resembled a thin black cord stretched along the leading edge. Stalling of the section, between 15° and 16°, was indicated by the sudden disappearance of the liquid filament, and a general forward flow of the liquid from about half chord towards the leading edge.

3.3 Normal Force and Pitching Moment

The normal force curve, obtained by integration of the pressure distributions, is linear up to 12° incidence with a slope 0.063 per degree (Fig. 4)*. Maximum lift at 15° is followed by an abrupt drop at 16°, but above this angle the decrease in normal force is comparatively gentle; $\bar{C}_{n_{max}}$ is 0.89.

The pitching moment coefficient about the section leading edge varies linearly with $\bar{C}_n$ almost up to $\bar{C}_{n_{max}}$ (Fig. 5). After stalling occurs, the curve turns back on itself and suddenly drops.

4. Discussion of Results

The leading edge type of stall is discussed by Gault and McCullough in Ref. 4, based on tests of the NACA 63-012 and 63-009 sections. Test results for the NACA 64A006 section are given in Ref. 2. All these N.A.C.A. tests were at a Reynolds number of about 5.8 million.

The pressure distributions obtained for the section under test exhibit the same features as those of the thin N.A.C.A. sections; the continual increase of peak negative pressures, followed by abrupt collapse at the leading edge and a redistribution of pressure along the chord. The slight dip in the curves near the leading edge after the peaks collapse is also present in all the tests, but is most marked with the 64A006 section; in the case of the test section a higher suction persists right at the leading edge, but it is clear that a similar phenomenon exists in both cases. Constant pressure regions further aft, as with the test section, also occur with the N.A.C.A. sections.

The lift curves also resemble each other, in that the N.A.C.A. sections show abrupt discontinuities when the angle of incidence for maximum lift is exceeded, the peaks of the curves being sharp.

The N.A.C.A. tests established that separation of the laminar boundary layer occurred near the nose and that flow re-attachment took place with a transitional type boundary layer which became turbulent within a short distance downstream. Laminar separation always occurred downstream of the pressure peak, and the relatively constant pressure region indicated the extent of the bubble, although pressure recovery began upstream of the point of flow re-attachment. The bubble forms well before the attainment of maximum lift, shortly after the leading edge pressure peak is formed: the separated layer appears to follow a path approximately tangential to the surface at the point of separation. Transition then occurs, and the expansion of the turbulent flow spreads at such an angle relative to the path of tangency of the separated laminar layer that the flow quickly re-attaches to the surface. Increase of incidence moves the pressure peaks nearer the leading edge, and because laminar separation is primarily a function of pressure recovery, the point of laminar separation also moves forward. The separation

and/

---

* This is a very small value for lift-curve slope, when compared to the value of 0.11 obtained in two-dimensional tests of similar sections, and indicates that the platforms, as already mentioned, were not effective in simulating infinite aspect ratio.

and transition thus occur in a region of increasing curvature of the aerofoil surface, and hence the transition point is progressively moving a greater distance above the surface. Stalling of the section presumably occurs when the transition point is so distant from the surface that the surface further aft does not lie within the wedge of turbulence, and the flow separates completely, with the accompanying abrupt collapse of the negative pressures at the leading edge.

This hypothesis implies that with increase of incidence the bubble region should progress towards the leading edge and become narrower, and in fact, measurements and liquid film studies for the 63-009 section indicate that at 4° the bubble lies between 0.008 and 0.014 chord, and moves forward steadily to between 0.003 and 0.006c at 8°. In spite of the similarities of the pressure distributions for the N.A.C.A. section and the present test section, a different state of affairs was indicated for the latter section with the liquid film study. As already described, the bubble appeared to be stationary up to 10° (Fig. 3), which would be expected from the fact that the pressure peaks were located about 0.02 chord for this incidence range. At 11° the pressure peak moved abruptly forward to the leading edge, and in agreement with the N.A.C.A. observations, the bubble formed immediately aft of the peak. This leaves the difficulty of interpreting the significance of the simultaneous lampblack accumulation in its original location about 0.025c at this particular incidence.

The persistence of a negative pressure right at the leading edge until complete separation, (Fig. 2), presumably indicates that some form of highly localized bubble vortex exists right on the leading edge, but it is difficult to see how this can originate without some initially attached layer. A possible explanation may lie in the results discussed by McCullough and Gault for thin aerofoil stall (Ref. 4); they tested a 4.23% thick double-wedge sharp-edged section, and found that even though separation occurred at the leading edge the mechanism is very different from that described above for the round-nosed sections. The flow appears to be unable to remain attached to the surface while passing from the stagnation point on the lower surface around the sharp leading edge to the upper surface. The theoretically infinite velocities at the sharp edge are physically impossible and the flow separates right at the leading edge. This separated flow passes above the surface and re-attaches further downstream. The boundary-layer velocity profile at the re-attachment point does not resemble a typical laminar or a typical turbulent profile, but gradually adjusts itself into a fully developed turbulent layer profile before reaching the trailing edge.

Tests of the NACA 64A006 section suggest that at low incidences the flow resembles that on the 63-009 section, with an initial laminar layer, separation, and turbulent re-attachment. At about 5° incidence the flow changes abruptly and conditions then resemble those on the sharp-edged section, with separation right at the leading edge and re-attachment some way aft. The pressure distribution curves for this section just before and after collapse of the peak suctions resemble those of the present test section in Fig. 2 for 15° and 16° very closely, and it would seem, therefore, that the flow characteristics of the test section follow the same trend as the NACA 64A006 section.

The behaviour of the flow round the leading edge may arise as follows. At 6° incidence there is laminar separation just aft of the peak suction at 0.02c (Fig. 3) with a bubble vortex formed underneath it and re-attachment about 0.04c. Conditions remain almost unchanged up to 9° incidence, but at 10° there is a very small separation region right at the nose, since the stagnation point is now well round the lower surface and the leading edge virtually presents a sharp edge to the flow. This flow, which is still laminar, very rapidly re-attaches to the surface, about 0.005c, but slightly further aft, about 0.02c, the conditions are such as to cause laminar separation and the formation of a bubble vortex. At 11° both régimes exist, and the lampblack accumulates in the highly localised separation region right at the leading edge and also in the bubble vortex further aft. At higher incidences, up to 15°, only leading edge separation occurs, as indicated by the filament of fluid right on the leading edge, followed by re-attachment. The collapse of the nose pressure peaks at 16° presumably coincides with the failure of the separated flow over the leading edge to re-attach.

Thus/

Thus it may be surmised that the first separation arises due to extremely high curvature in accelerated flow at the leading edge, while the second further aft is produced by the deceleration. It does not seem unreasonable to assume, therefore, that because of the favourable pressure gradient the flow which separated at the leading edge would be quite likely to remain laminar, and re-attach in that state, whereas after the second separation the adverse gradient would almost immediately cause transition.

Further investigation of the flow in the vicinity of the leading edge will be required before the explanation of the flow behaviour suggested above can be accepted, and tests at a much higher Reynolds number would be desirable.

Some Japanese experiments on the effects on laminar separation of body surface geometry, Reynolds number (based on length between the points of separation and re-attachment), stream turbulence, and a transition wire mounted at various heights above the point of separation have been reported[5]. A bent plate was mounted in a wind tunnel with the sharp bend normal to the stream. The laminar flow over the forward portion of the plate, which was at some negative incidence, separated at the edge of the bend and re-attached further aft on the rear portion of the plate, which was at some positive incidence. A bubble vortex was formed just downstream of the bent edge; pitot and static tube traverses of the bubble were made, and it was also studied visually with the lampblack technique.

With the plate set at a forward incidence of -9.5° and a rearward incidence of 7°, measurements were made at wind-speeds of 26.6 and 50 ft per sec. At the lower speed there was a region of lampblack at rest extending aft from the bent edge, followed by a region of accumulated lampblack, which ended in the sharp line denoting reversed flow. Increase of speed caused the region of lampblack at rest to disappear, and the region of accumulation and the starting line of reverse flow both moved upstream. The dynamic pressure was zero at the bent corner as the bubble was crossed, became negative, then increased suddenly, reaching a maximum and finally decreased gradually. The downstream edge of lampblack accumulation coincided with the position where the dynamic pressure began to increase, and the starting line of reverse flow coincided with the position of maximum dynamic pressure. The static pressure distribution also changed with speed: at the higher speed the negative pressure coefficient at the bent corner almost doubled, and in agreement with the lampblack indications, the "flat" portion of the distribution was very much narrower, showing that the bubble was reduced in chordwise extent.

It would appear, therefore, that there is a considerable Reynolds number effect on the extent of the bubble, since in both cases the separation point was fixed at the bent edge.

After separation the turbulence of the layer spreads at an angle which increases with free stream turbulence. Thus, with a more turbulent free stream, the point of re-attachment was closer to the bent edge. The transition wire above the bent edge also brought the point of re-attachment forward, the effect decreasing as the height of the wire above the corner was increased.

4.1 Relation to Three-dimensional Tests

One of the most significant features of the two-dimensional tests is the abrupt change in the nature of the pressure distributions between 10° and 11° incidence. This was the incidence range for the wing model at which the bubble vortex lying spanwise abruptly swung aft. Outboard of this change of direction, a thin filament of fluid was observed along the leading edge, which was described in Part I of this report as the growth of a new separation vortex.

It would appear from these two-dimensional results that on the wing the vortex must either be located about 0.02c, as it is up to 10°, or if the wing section is effectively at a higher incidence, it must jump forward to lie along the leading edge. This would account for the fact that when the wing was oscillated gently from 9° to 11°, with the region of vortex change-of-direction kept covered in liquid, it was impossible to maintain a bifurcated accumulation of fluid.

Either/

Either there was a continuous spanwise band of fluid located about 0.02c, from root to tip, or else there was the band curving aft about mid span, and the fluid outboard of that moving forward rapidly to accumulate at the leading edge.

This knowledge still does not help to make clear the actual mechanism of the abrupt change of direction of the bubble vortex, but it does at least suggest strongly that the leading edge vortex formed further outboard arises from sectional characteristics, and is not peculiar to a sweptback wing.

5. Conclusions

Pressure distribution and liquid-film tests have shown that the sectional characteristics of the 10% thick aerofoil section used on the swept-wing model are governed largely by flow conditions in the vicinity of the leading edge.

At incidences up to 10° the laminar boundary layer over the nose separates, becomes transitional away from the surface, and re-attaches as a turbulent layer, a bubble vortex forming under the separated layer. Above 10° the characteristics alter and the flow behaves rather as if the leading edge were sharp, with a separation immediately at the edge itself. This separated flow re-attaches further aft, up to 15° incidence, but at greater incidences it remains separated and the section is stalled.

Further investigation of flow conditions over the leading edge are required before the mechanism can be fully understood. Factors such as Reynolds number, surface roughness, nose radius and stream turbulence could influence the behaviour of the boundary layer in this region, but no deductions as to their relative effect can be made at present on the basis of these limited tests.

References

No.	Author(s)	Title, etc.
1	Donald E. Gault	Boundary-layer and stalling characteristics of the NACA 63-009 airfoil section. N.A.C.A. Technical Note No. 1894. (June, 1949). A.R.C. 12,780
2	George B. McCullough and Donald E. Gault	Boundary-layer and stalling characteristics of the NACA 64A006 airfoil section. N.A.C.A. Technical Note No. 1923. (August, 1949). A.R.C. 12,781
3	W. J. Bursnall and L. K. Loftin	Experimental investigation of localised regions of laminar-boundary layer separation. N.A.C.A. Technical Note No. 2338, April 1951.
4	G. B. McCullough and D. E. Gault	Examples of three representative types of airfoil section stall at low speed. N.A.C.A. Technical Note No. 2502, September, 195
5	T. Maekawa and S. Atsumi	Transition caused by laminar flow separation. Jour. Soc. Applied Mechs. Japan, Vol. 1, No. 6, November, 1948. Trans. as N.A.C.A. Tech. Memo. No. 1352, September, 1952.

JC.

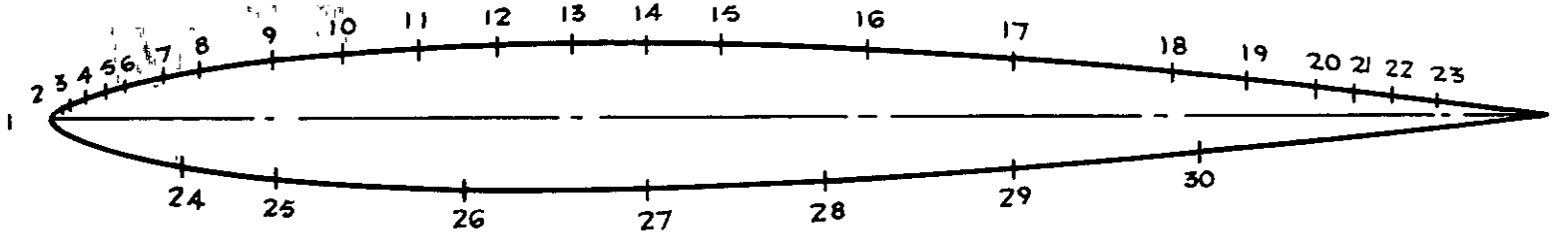

The Aerofoil showing Location of Pressure Holes

FIG 1.

FIG 2

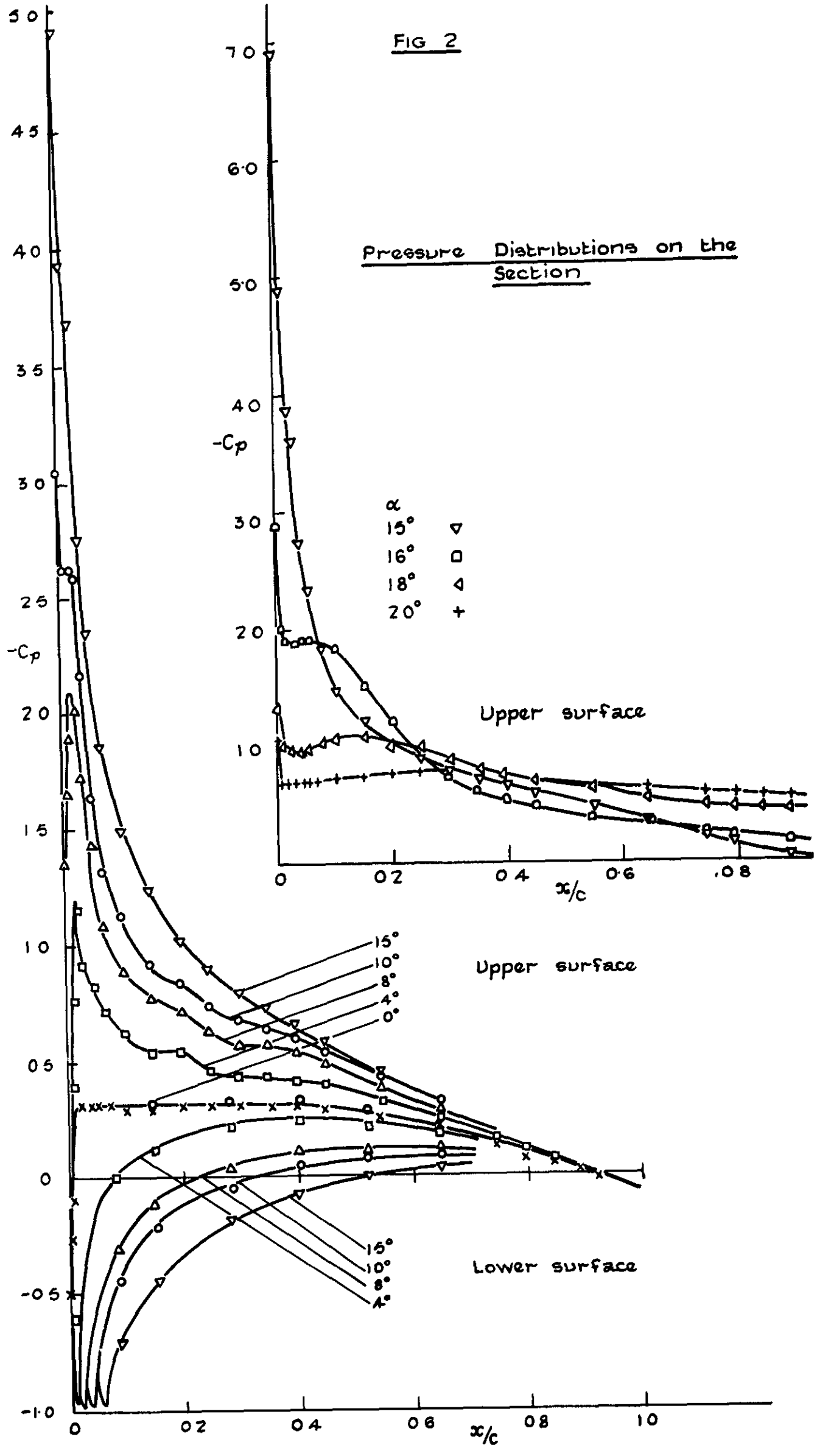
Pressure Distributions on the Section
-Cp
α
15°
16°
18°
20°
Upper surface
x/c
15°
10°
8°
4°
0°
Upper surface
15°
10°
8°
4°
Lower surface
x/c

FIG 3

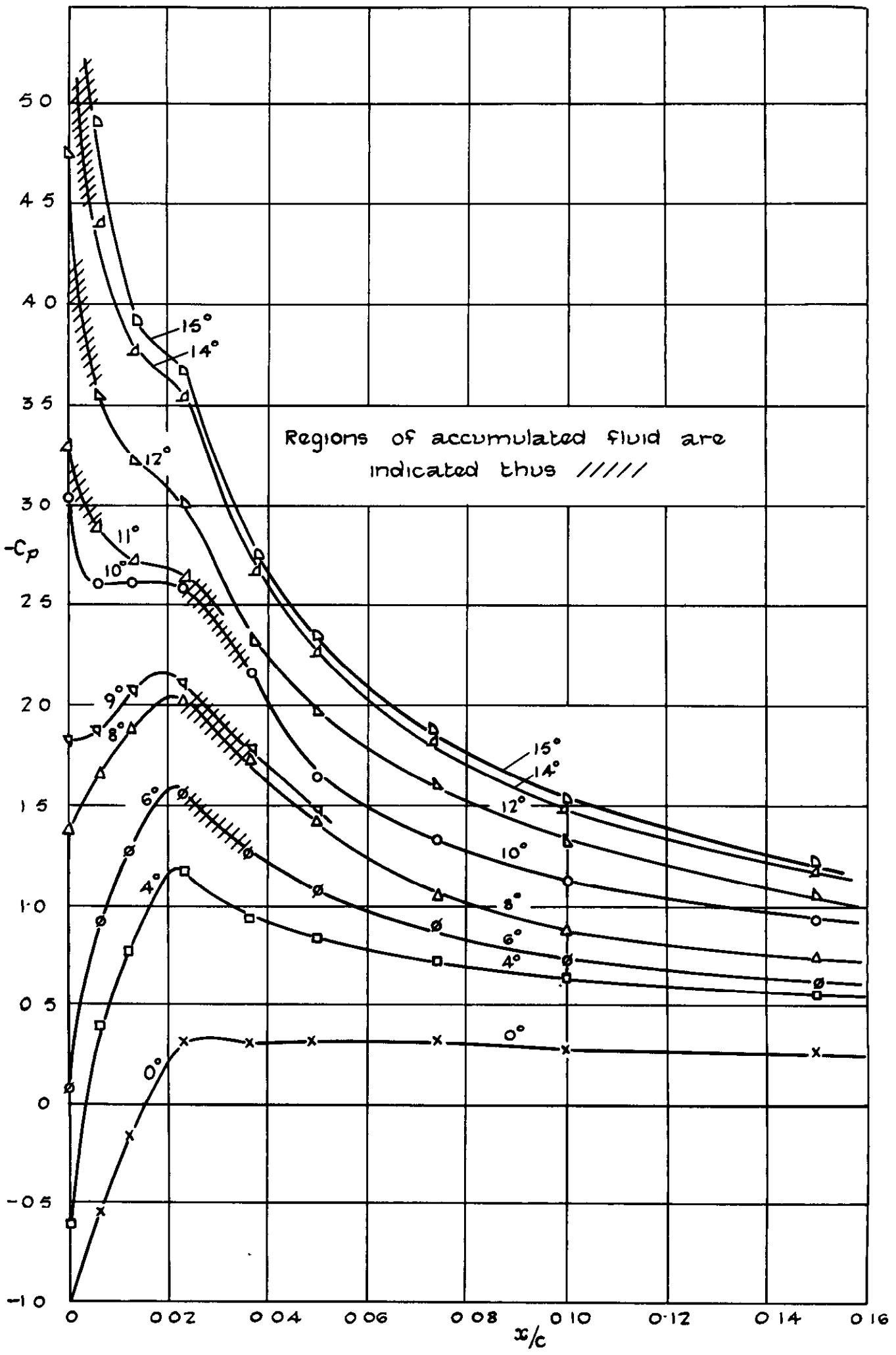

Pressure Distributions in the Vicinity of the Leading Edge.

FIG 4

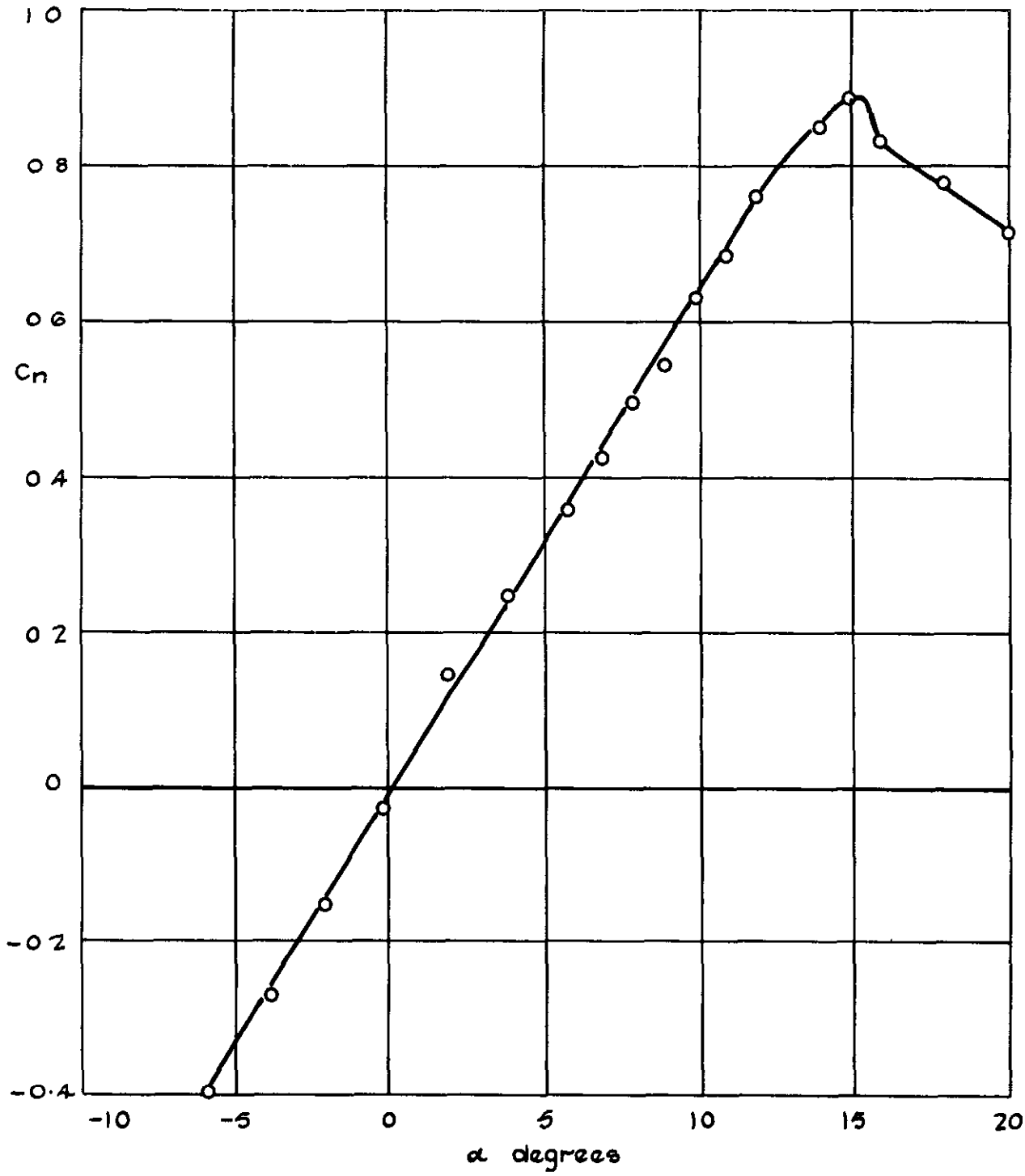

Variation of Normal Force Coefficient with Incidence.

FIG 5

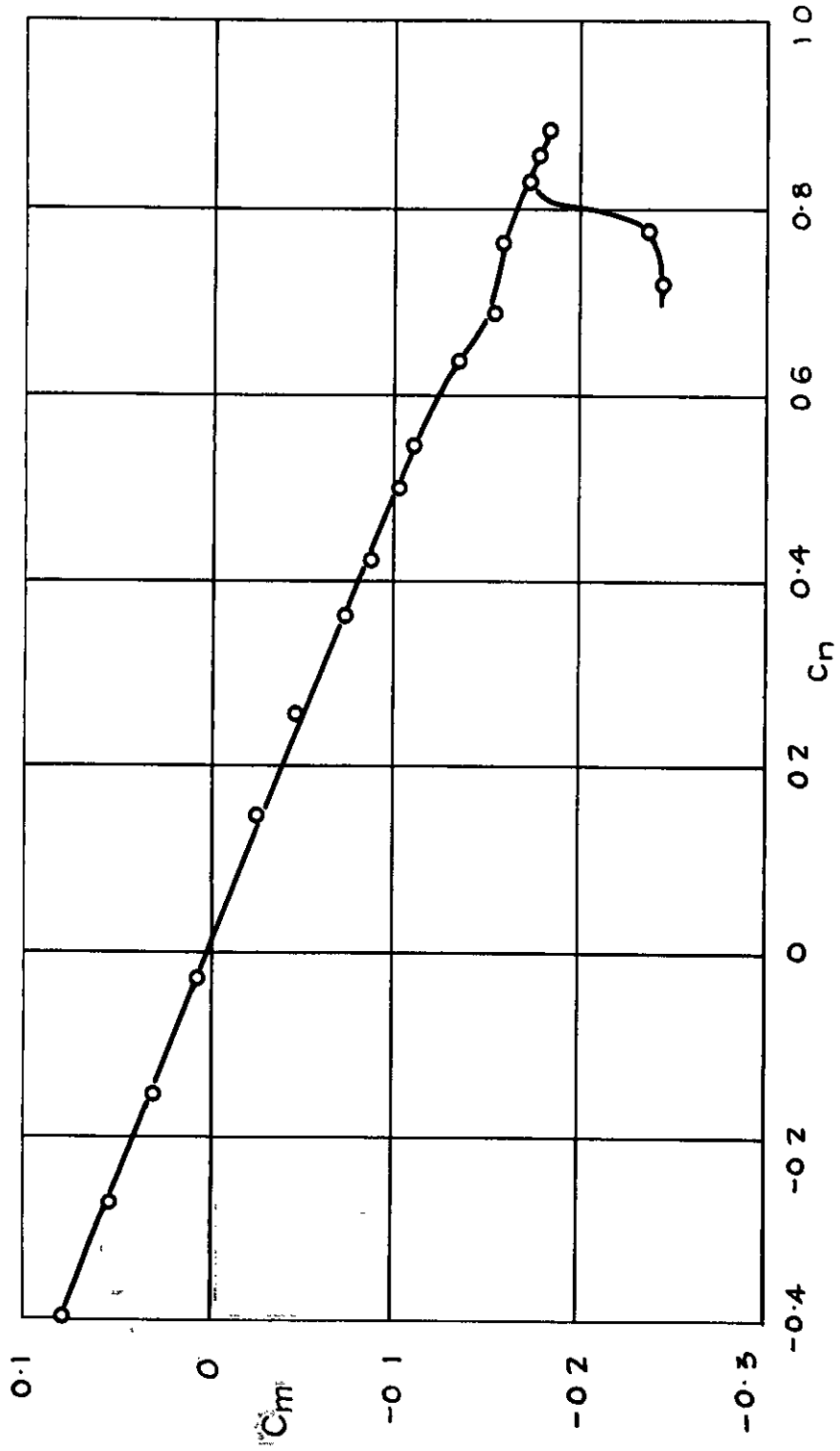

Variation of Pitching Moment Coefficient with C_n

C.P. No. 137
(15,437 15,524)
A R.C Technical Repor

PRINTED AND PUBLISHED BY HER MAJESTY'S STATIONERY OFFICE
To be purchased from
York House, Kingsway, LONDON, W C 2 429 Oxford Street, LONDON, W 1
P O Box 569, LONDON, S E 1
13a Castle Street, EDINBURGH, 2 1 St. Andrew's Crescent, CARDIFF
39 King Street, MANCHESTER, 2 Tower Lane, BRISTOL, 1
2 Edmund Street, BIRMINGHAM, 3 80 Chichester Street, BELFAST
or from any Bookseller
1953
Price 8s 6d net
PRINTED IN GREAT BRITAIN

23—9007—
S O Code No.